



Biogeochemical Modelling of Ria Formosa (South Coast of Portugal) with EcoDynamo Model description



Pedro Duarte, António Pereira, Manuela Falcão, Dalila Serpa, Catarina Ribeiro, Rui Bandeira and Bruno Azevedo

University Fernando Pessoa, Centre for Modelling and Analysis of Environmental Systems

June 2006

DITTY (Development of an information technology tool for the management of Southern European lagoons under the influence of river-basin runoff) (EESD Project EVK3-CT-2002-00084)

Summary

In this work a biogeochemical model of Ria Formosa (South of Portugal) is presented. Ria Formosa is a large (c.a. 100 km²) mesotidal lagunary system with large intertidal areas and several conflicting uses, such as fisheries, aquaculture, tourism and nature conservation. This coastal ecosystem is a natural park where several management plans and administrative responsibilities overlap.

The work presented here is part of a coupled hydrodynamic-biogeochemical model that includes pelagic and benthic processes and variables. It is a two-dimensional vertically integrated model, based on a finite differences grid with a 100 m spatial step and a semi-implicit resolution scheme. It is forced by conditions at the sea boundary, river and water treatment plant discharges, wind speed, light intensity and air temperature. The model includes a wet-drying scheme to account for the dynamics of the large intertidal areas.

The purposes of this work are to describe the biogeochemical model and how it has been coupled with a hydrodynamic model, discuss its structure and present some calibration exercises.

CONTENTS

1	Introduction	1
1.1	Site description	1
1.2	Objectives	2
2	Methodology.....	2
2.1	Model software description and implementation	3
2.2	Biogeochemical model description	8
2.2.1.	Hydrodynamic object	24
2.2.2.	Wind object.....	24
2.2.3.	Air temperature object	24
2.2.4.	Light intensity and water temperature objects.....	24
2.2.5	Dissolved substances object	24
2.2.6	Suspended matter object.....	25
2.2.7	Phytoplankton object	26
2.2.8	<i>Enteromorpha</i> spp. and <i>Ulva</i> spp. objects	27
2.2.9	<i>Zostera noltii</i> object.....	27
2.2.10	<i>Ruditapes decussatus</i> object	27
2.3	Model setup	28
2.4	Model testing	31
3	Results and discussion	32
4	References	44

1 Introduction

This work is part of the DITTY project “Development of an Information Technology Tool for the Management of European Southern Lagoons under the influence of river-basin runoff” (<http://www.dittyproject.org/>). The general objective of DITTY is the development of information technology tools integrating Databases, Geographical Information Systems (GIS), Mathematical Models and Decision Support Systems to help in the management of southern European coastal lagoons and adjacent watersheds, within the objectives of the Water Framework Directive (UE, 2000).

The DITTY project takes place at five southern European coastal lagoons. The work presented here concerns the biogeochemical modelling of Ria Formosa – the Portuguese case study within DITTY (Fig. 1-1).

1.1 *Site description*

Ria Formosa is a shallow mesotidal lagoon located at the south of Portugal (Algarve coast) with a wet area of 10 500 ha (Figure 1-1). The lagoon has several channels and a large intertidal area, which corresponds roughly to 50% of the total area, mostly covered by sand, muddy sand-flats and salt marshes. The intertidal area is exposed to the atmosphere for several hours, over each semi-diurnal tidal period, due to its gentle slopes. Salinity remains close to 36 ppt, except during sporadic and short periods of winter run-off. Tidal amplitude varies from 1 to 3.5 meters and the mean water depth is 3.5 m.

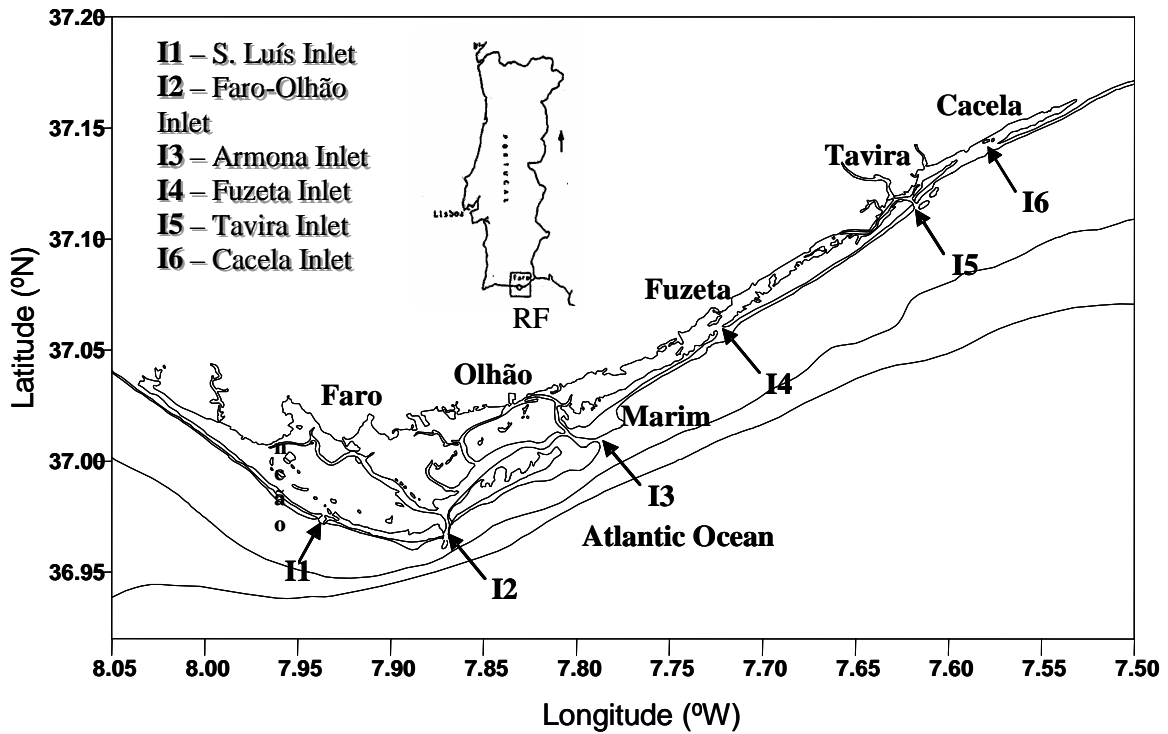


Figure 1-1- Geographic location of Ria Formosa and its inlets (I1 – I6).

1.2 Objectives

The purposes of this work are to describe a biogeochemical model implemented for Ria Formosa and how it has been coupled with a hydrodynamic model, discuss its structure and present some calibration exercises.

2 Methodology

The biogeochemical model implemented in this work is a two dimensional vertically integrated model based on a finite difference staggered grid, as described previously for the hydrodynamic model (cf. – Duarte et al, 2005), that calculates the velocity field with the equations of motion and the equation of continuity (Knauss, 1997) and solves the transport equation for all pelagic variables:

$$\frac{dS}{dt} + \frac{\partial(uS)}{\partial x} + \frac{\partial(vS)}{\partial y} = A_x \frac{\partial^2 S}{\partial x^2} + A_y \frac{\partial^2 S}{\partial y^2} + Sources - Sinks \quad (1)$$

Where,

u and v - current speeds in x (West-East) and y (South-North) directions (m s^{-1}); A – Coefficient of eddy diffusivity ($\text{m}^2 \text{s}^{-1}$); S – A conservative (Sources and Sinks are null) or a non conservative variable in the respective concentration units.

The biogeochemical model provides the values for the *Sources* and *Sinks* terms of equation 1 at each grid cell.

2.1 Model software description and implementation

The model was implemented using EcoDynamo (Pereira & Duarte, 2005). EcoDynamo uses Object Oriented Programming (OOP) to relate a set of "ecological" objects by means of a server or shell, which allows these to interact with each other, and displays the results of their interaction. Both the EcoDynamo shell and the objects have been programmed in C++ for Windows™. There are different objects to simulate hydrodynamic, thermodynamic and biogeochemical processes and variables. The shell interface allows the user to choose among different models and to define the respective setups – time steps, output formats (file, graphic and tables), objects to be used and variables to be visualised. The objects used in the present model are listed in Table 2-1 and described below. The physical and biogeochemical processes simulated by the model are presented in Figs. 2-2 and 2-3. Differential equations for water column, pore water, sediment and benthic variables are shown in Tables 2-2 – 2-5. Part of these equations (those concerning pelagic state variables), represent the *sources-sinks* terms of Equation 1. The corresponding rate equations are presented in Tables 2-6 – 2-9. Model parameters are listed in Table 2-10.

Table 2-1 – EcoDynamo objects implemented for Ria Formosa and respective variable outputs (see text).

Object type	Object name	Object outputs
Objects providing forcing functions	Wind object	Wind speed
	Air temperature object	Air temperature
	Water temperature object	Radiative fluxes and balance between water and atmosphere and water temperature
	Light intensity object	Total and photosynthetically active radiation (PAR) at the surface and at any depth
	Tide object	Tidal height
	Salt marsh object	Nitrate consumption, ammonia and suspended matter release
Objects providing state variables	Hydrodynamic 2D object	Sea level, current speed and direction
	Sediment biogeochemistry object	Pore water dissolved inorganic nitrogen (ammonia, nitrate and nitrite), inorganic phosphorus and oxygen, sediment adsorbed inorganic phosphorus, organic phosphorus, nitrogen and carbon
	Dissolved substances object	Dissolved inorganic nitrogen (ammonia, nitrate and nitrite), inorganic phosphorus and oxygen
	Suspended matter object	Total particulate matter (TPM), particulate organic matter (POM), carbon (POC), nitrogen (PON), phosphorus (POP) and the water light extinction coefficient
	Phytoplankton object	Phytoplankton biomass, productivity and cell nutrient quotas
	<i>Enteromorpha sp.</i> object	Macroalgal biomass, productivity and cell nutrient quotas
	<i>Ulva sp.</i> object	Macroalgal biomass, productivity and cell nutrient quotas
	<i>Zostera noltti</i> object	Macrophyte biomass and numbers, cell nutrient quotas and demographic fluxes
	Clams (<i>Ruditapes decussatus</i>) object	Clam size, biomass, density, filtration, feeding, assimilation and scope for growth

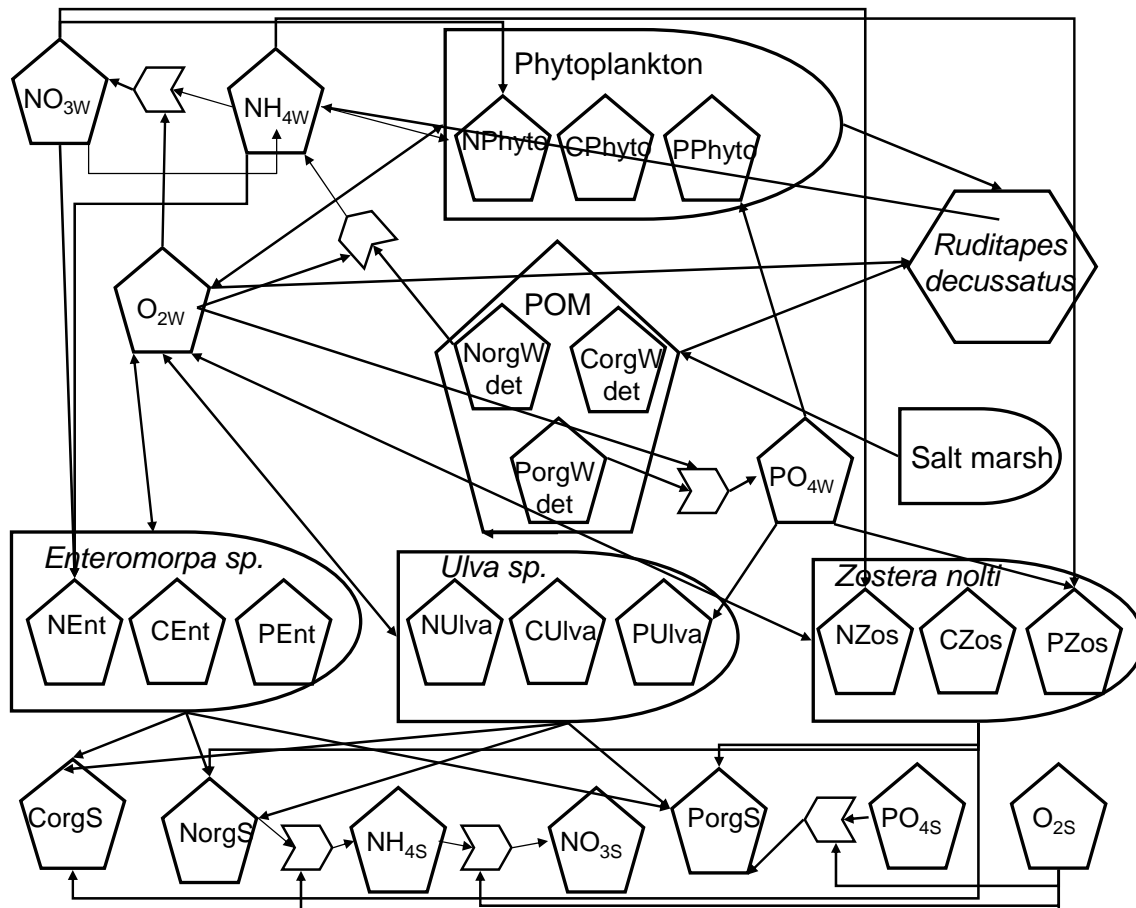


Fig. 2-1 - Biogeochemical processes and variables simulated by the model. The name of the variables is the same as in Tables 2-2 – 2-8. The prefix N, C, and P refers to Nitrogen, Carbon and Phosphorus. The subscripts *w* and *s* refer to water column or sediment variables.

Given the large intertidal areas of Ria Formosa (cf. – 1.1 Site description), the model includes a wet-drying scheme that prevents any grid cell from running completely dry, avoiding numerical errors. The general approach is to stop using the advection term when depth is lower than a threshold value (0.1 m in the present case) to avoid numerical instabilities. Below this threshold and until a minimum limit of 0.05 m, the model computes all remaining terms. When this limit is reached, computations do not take place in a given cell until a neighbour cell has a higher water level, allowing then the pressure term to start “filling” the “dry” cell.

This hydrodynamic model is forced by water level and river discharges at sea and land boundaries, respectively. The former are calculated by the equations and the harmonic components for the Faro-Olhão harbour (cf. – Fig.1-1) described in SHOM (1984) and listed in a previous report (Duarte et al., 2005). Biogeochemical processes are forced by

sea-lagoon exchanges, river discharges, air-water heat and mass exchanges and light intensity.

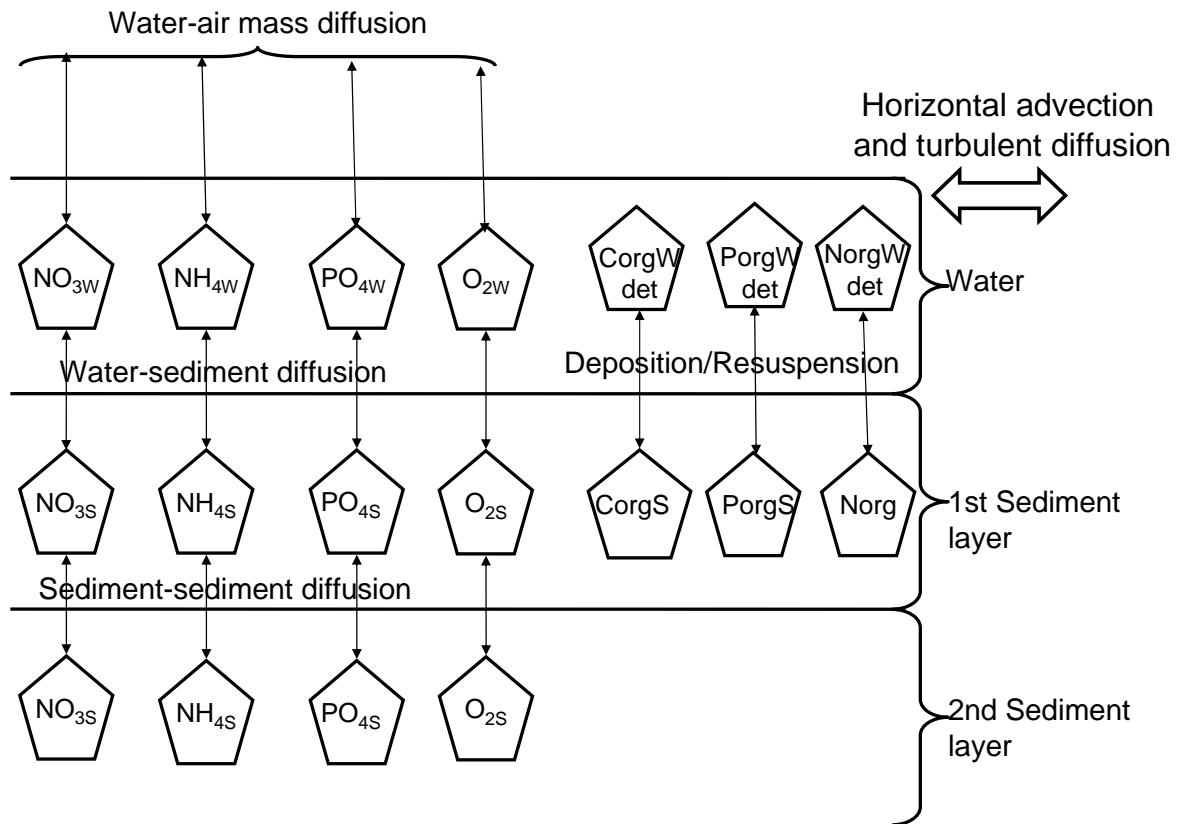


Fig. 2-2 - Physical and biogeochemical processes and variables simulated by the model. The name of the variables is the same as in Tables 2 – 5. The prefix N, C, and P refers to Nitrogen, Carbon and Phosphorus. The subscripts *w* and *s* refer to fluxes in the water column or in sediment layers.

The wet-drying scheme referred above requires a relatively high spatial and temporal resolution. In the present case, the former is 100 m and the latter 3 s. A lower temporal resolution leads to numerical errors, in spite of the semi-implicit numerical scheme of the hydrodynamic model (Duarte et al., 2005). Therefore, the model requires a large computing time. Several steps were taken to reduce the computational costs: (i) To subdivide Ria Formosa in two subsystems – the western and the eastern Ria - as described in a previous report (Duarte et al., 2005); (ii) To run biogeochemistry only for the part of the model domain covering the precise area of Ria Formosa; (iii) To run only the hydrodynamic part of the model, save the results and “rewind” them later to provide

the hydrodynamic forcing for the biogeochemical simulations (cf. - 2.2.1 Hydrodynamic object) and (iv) To produce a multi- processing version of EcoDynamo.

In what concerns the first step, Ria Formosa was indeed sub-divided. In the present work it was considered only the “Western Ria” (Fig. 2-3).

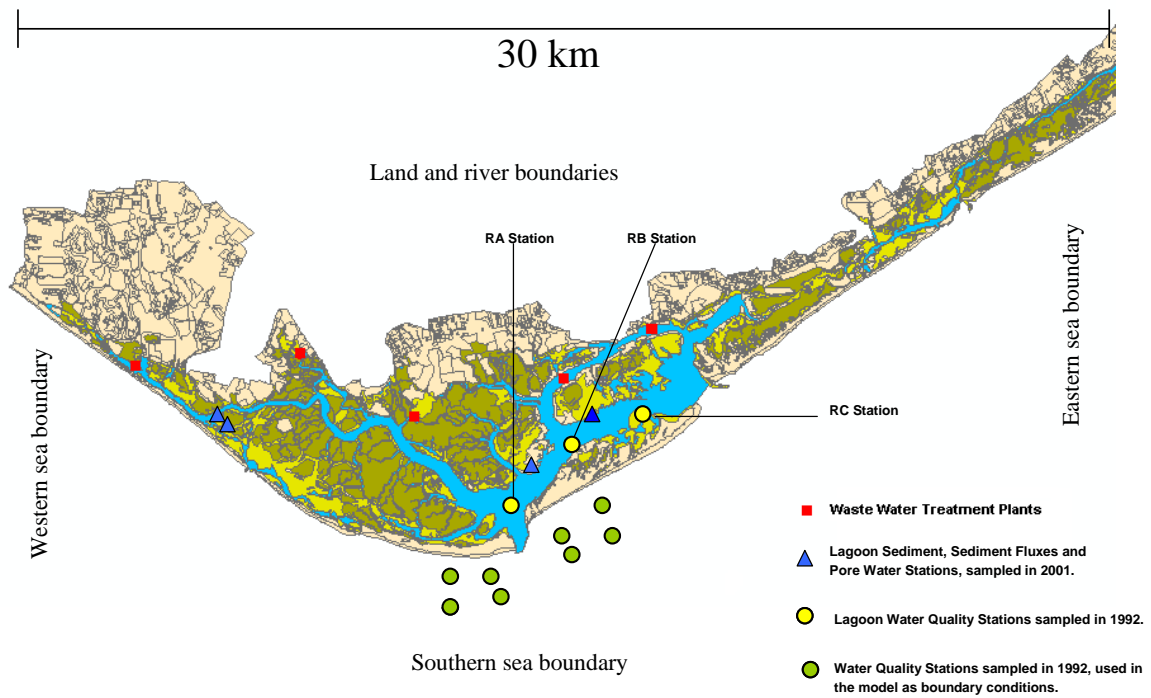


Fig. 2-3 – Model domain covering a total area of 546 km² (whole rectangle) and 98 km² (only the area of covered by the lagoon), for the hydrodynamic and biogeochemical simulations, respectively. Spatial resolution is 100 mm. Time step is 3 and 30 seconds for the hydrodynamic and the biogeochemical simulations, respectively (see text). Regarding the second step, it is possible to run only a part of the model domain, by defining a sub-domain, allowing a much faster simulation of biogeochemical processes. In the present case, sub-domain shape matches exactly the shape of the Western Ria Formosa. However, current velocity data must be available for transport calculations (equation 1) (cf. - 2.2.1 Hydrodynamic object). Pereira & Duarte (2005) describe how to run a sub-domain with the EcoDynamo shell. Rodrigues et al. (2005) describe how to produce a text file of coordinates using ArcGIS that may be handled with EcoDynamo as a sub-domain.

In what concerns the third item, there are two main different running modes in EcoDynamo – one with an online coupling of hydrodynamic and biogeochemical processes and another with an offline coupling. The latter uses previously obtained and

time integrated (for 5 minute periods in the present case) data series of current flows with the hydrodynamic object, to transport water properties among model grid cells. This allows for a faster simulation, avoiding the computation overhead of hydrodynamic processes and the small time steps generally required. This simplified mode was used in the present work. Whereas “online coupling” needs a 3 s time step for stability restrictions, mostly because of very low depths over intertidal areas, the offline simulations may use a time step of up to 60 s. In fact, a variable time step is used, so that sites where instabilities may arise are resolved with more detail and properly time integrated with neighbour cells. Instabilities generally occur when the volume in a cell is very low. In this case, if the time step is not small enough, the computed flow across one of the cell “walls” times the time step, may be larger than cell volume. When calculating transport of salt or any other property, this situation may lead to the violation of mass conservation. The algorithm consists in resolving with more detail these “critical cells” and their interactions with neighbour cells, finding a time step small enough to prevent mass conservation violations and numerical instabilities.

Regarding the multi-processing version of EcoDynamo, it handles different objects has different threads, meaning that they may run in different processors. This implied to synchronize the objects. The transport equation (equation 1) must be solved only after all pelagic objects (see below) calculate their source and sink terms, because some of these terms depend on state variables of other objects.

2.2 Biogeochemical model description

Differential equations used for suspended matter dynamics and biogeochemical processes are shown in Tables 2-2 – 2-5. Part of these equations (those concerning pelagic state variables), represent the *sources-sinks* terms of Equation 1. The corresponding rate equations are presented in Tables 2-6 – 2-8. Model parameters are listed in Table 2-9.

The model includes the pelagic and the benthic compartment as well as their interactions. Pelagic variables are water temperature and those depicted in Tables 2-2 and 2-4 – dissolved nutrients, suspended matter and phytoplankton. Benthic variables

are those listed in Tables 2-3 and 2-5. In the case of suspended matter, it is noteworthy that carbon, nitrogen and phosphorus concentrations are computed simultaneously. The same is true for the sediments. The benthic compartment is divided in two vertical layers (Fig. 2-2). The height of the top layer may increase or decrease according to the net result of deposition and resuspension.

For a description of objects providing forcing functions and the hydrodynamic object (cf. – Table 2-1) refer Duarte et al. (2003) and Duarte et al. (2005). Salt marsh object acts merely as a nitrate sink and an ammonium and particulate organic matter source, according to experimental data obtained by Falcão (unpublished). It is assumed that nitrate-nitrogen input equals ammonium-nitrogen output. This influx/outflux occurs along the salt marsh boundaries (Fig. 2-1). The model is also forced by WTP discharges regarding suspended matter and nutrient loads.

Table 2-2 – General differential equations for water column dissolved inorganic nitrogen, phosphorus and oxygen. The subscripts *i* and *j* refer to the line and columns of the model grid. These differential equations only describe changes due to non-conservative processes and provide the *sources-sinks* terms of Equation 1. The load terms refer to loads along the sea, river and land boundaries.

Water column ammonium (NH₄) (μmol N l⁻¹)		
$\frac{dNH_{4ij}}{dt} = PONMinerW_{ij} - NitrificationW_{ij} + DeNitrificationW_{ij} \pm SedWaterDiffusionNH_{4ij} + BIVExcrNH_{4ij} - PhyUpNH_{4ij} - EntUpNH_{4ij} - UlvUpNH_{4ij} - ZosUpNH_{4ij} + loadsNH_{4ij}$		
Mineralization, nitrification and denitrification as in Chapelle (1995).		
<i>PONMinerW_{ij}</i>	Water column particulate organic nitrogen mineralization	
<i>NitrificationW_{ij}</i>	Water column nitrification	
<i>DeNitrificationW_{ij}</i>	Water column denitrification	
<i>SedWaterDiffusionNH_{4ij}</i>	Sediment-water diffusion	μmol N l ⁻¹ time ⁻¹
<i>BIVExcrNH_{4ij}</i>	Clams excretion	
<i>PhyUpNH_{4ij}</i>	Uptake by phytoplankton	
<i>EntUpNH_{4ij}</i>	Uptake by <i>Enteromorpha sp.</i>	
<i>UlvUpNH_{4ij}</i>	Uptake by <i>Ulva sp.</i>	
<i>ZosUpNH_{4ij}</i>	Uptake by <i>Zostera noltii</i> leaves	
<i>loadsNH_{4ij}</i>	Nitrogen loads	

Water column nitrate+nitrite (NO) ($\mu\text{mol N l}^{-1}$)

$$\begin{aligned} \frac{dNO_{ij}}{dt} = & \text{Nitrification}W_{ij} - \text{Denitrification}W_{ij} \pm \text{SedWaterDiffusion}NO_{ij} \\ & - \text{PhyUp}NO_{ij} - \text{EntUp}NO_{ij} - \text{UlvUp}NO_{ij} - \text{ZosUp}NO_{ij} \\ & + \text{loads}NO_{ij} \end{aligned}$$

(3)

The fluxes for the uptakes have the same prefix as for ammonia to indicate the species or species group responsible for each uptake. Their units are $\mu\text{mol N l}^{-1} \text{ time}^{-1}$.

Water column phosphate (PO₄) ($\mu\text{mol P l}^{-1}$)

$$\begin{aligned} \frac{dPO_{4ij}}{dt} = & \text{POPMiner}W_{ij} \pm \text{SedWaterDiffusion}PO_{4ij} \\ & - \text{PhyUp}PO_{4ij} - \text{EntUp}PO_{4ij} - \text{UlvUp}PO_{4ij} - \text{ZosUp}PO_{4ij} \\ & + \text{loads}PO_{4ij} \end{aligned} \tag{4}$$

The fluxes for the uptakes have the same prefix as for ammonia and nitrate to indicate the species or species group responsible for each uptake. Their units are $\mu\text{mol P l}^{-1} \text{ time}^{-1}$.

<i>POPMiner</i> W _{ij}	Water column particulate organic phosphorus mineralization
---------------------------------	--

Water column dissolved oxygen (DO) ($\text{mg O}_2 \text{ l}^{-1}$)

$$\begin{aligned} \frac{dDO_{ij}}{dt} = & \pm \text{SedWaterDiffusion}_{ij} + \text{Kar} \left(DO_{satij} - DO_{ij} \right) \\ & - \text{BIVResp}_{ij} + \text{PhyPHOT}_{ij} - \text{PhyResp}_{ij} \\ & + \text{EntPHOT}_{ij} - \text{EntResp}_{ij} \\ & + \text{UlvPHOT}_{ij} - \text{UlvResp}_{ij} \\ & + \text{ZosPHOT}_{ij} - \text{ZosResp}_{ij} \\ & - \text{NitrificationCons}W_{ij} - \text{MineralizationCons}W_{ij} \end{aligned} \tag{5}$$

Raeration coefficient calculated as a function of wind speed as in Burns (2000). Oxygen consumption by nitrification and mineralization as in Chapelle (1995) and Chapelle et al. (2000).

<i>Kar</i>	Gas transfer/raeration coefficient	time^{-1}
<i>DO</i> _{satij}	Dissolved oxygen saturation concentration	$\text{mg O}_2 \text{ l}^{-1}$
<i>BIVResp</i> _{ij}	Bivalve respiration	
<i>PhyPHOT</i> _{ij}	Phytoplankton photosynthesis	
<i>PhyResp</i> _{ij}	Phytoplankton respiration	
<i>EntPHOT</i> _{ij}	<i>Enteromorpha sp.</i> photosynthesis	
<i>EntResp</i> _{ij}	<i>Enteromorpha sp.</i> respiration	
<i>UlvPHOT</i> _{ij}	<i>Ulva sp.</i> photosynthesis	$\text{mg O}_2 \text{ l}^{-1} \text{ time}^{-1}$
<i>UlvResp</i> _{ij}	<i>Ulva sp.</i> respiration	
<i>ZosPHOT</i> _{ij}	<i>Zostera noltii</i> photosynthesis	
<i>ZosResp</i> _{ij}	<i>Z. noltii</i> above ground respiration	
<i>NitrificationCons</i> W _{ij}	Consumption by water column nitrification	
<i>MineralizationCons</i> W _{ij}	Consumption by water column mineralization	

Table 2-3 - General differential equations for pore water variables – pore water ammonium, nitrate+nitrite, phosphate and oxygen – and sediment variables – organic carbon, nitrogen and phosphorus. The subscripts *i* and *j* refer to the line and columns of the model grid.

Pore water ammonium (NH_{4s}) (μmol N l⁻¹)		
$\frac{d NH_{4sij}}{dt} = \frac{OrgNMinerS_{ij}SedWaterRatio_{ij}}{NAtomicMass} - NitrificationS_{ij} + DeNitrificationS_{ij} \pm SedWaterDiffusionNH4_{ij} - ZosRootNH4S_{ij}$		
(6)		
<i>OrgNMinerS_{ij}</i>	Mineralization of sediment organic nitrogen	μg g ⁻¹ N time ⁻¹
<i>SedWaterRatio_{ij}</i>		g l ⁻¹
<i>NitrificationS_{ij}</i>	Pore water nitrification	
<i>DeNitrificationS_{ij}</i>	Pore water denitrification	
<i>SedWaterDiffusionNH4_{ij}</i>	Sediment-water diffusion	μmol N l ⁻¹ time ⁻¹
<i>ZosRootUpNH4S_{ij}</i>	Uptake by <i>Zostera noltii</i> roots	

Pore water nitrate+nitrite (NOs) (μmol N l⁻¹)		
$\frac{d NOS_{ij}}{dt} = NitrificationS_{ij} \pm SedWaterDiffusionNOs_{ij} - DenitrificationS_{ij}$		
(7)		
Nitrification and denitrification as in Chapelle (1995).		

Pore water phosphate (PO_{4s}) (μmol N l⁻¹)		
$\frac{d PO_{4sij}}{dt} = \frac{OrgPMinerS_{ij}SedWaterRatio_{ij}}{PAtomicMass} \pm SedWaterDiffusion_{ij} - SedimentAdsorption_{ij} + SedimentDesorption_{ij} - ZosRootUpPO4S_{ij}$		
(8)		
Adsorption and desorption as in Chapelle (1995).		
<i>OrgPMinerS_{ij}</i>	Mineralization of sediment organic phosphorus	μg g ⁻¹ N time ⁻¹
<i>ZosRootUpNH4S_{ij}</i>	Uptake by <i>Z. noltii</i> roots	μmol P l ⁻¹ time ⁻¹

Pore water oxygen (DO) (mg l⁻¹)		
$\frac{d DO_{ij}}{dt} = \pm SedWaterDiffusion_{ij} - ZosRootResp_{ij} - NitrificationConsS_{ij} - MineralizationConsS_{ij}$		
(9)		
<i>ZosRootResp_{ij}</i>	<i>Z. noltii</i> below ground respiration	
<i>NitrificationConsS_{ij}</i>	Consumption by pore water nitrification	mg O ₂ l ⁻¹ time ⁻¹
<i>MineralizationConsS_{ij}</i>	Consumption by pore water mineralization	

OrgN ($\mu\text{g N g}^{-1}$)		
$\frac{d\text{OrgN}_{ij}}{dt} = \text{DetrDepN}_{ij} + \text{PhySetN}_{ij} - \text{OrgNMinerS}_{ij} \quad (10)$		
DetrDepN_{ij}	Deposition of particulate nitrogen	
PhySetN_{ij}	Settling of phytoplankton cells	$\mu\text{g N g}^{-1} \text{ time}^{-1}$
OrgP ($\mu\text{g P g}^{-1}$)		
$\frac{d\text{OrgP}_{ij}}{dt} = \text{DetrDepP}_{ij} + \text{PhySetP}_{ij} - \text{OrgPMinerS}_{ij} \quad (11)$		
DetrDepP_{ij}	Deposition of particulate nitrogen	
PhySetP_{ij}	Settling of phytoplankton cells	$\mu\text{g P g}^{-1} \text{ time}^{-1}$
Adsorbed PO_4 ($\mu\text{g P g}^{-1}$)		
$\frac{d\text{PO}_{4\text{Ads}}_{ij}}{dt} = \left(\text{SedimentAdsorption}_{ij} - \text{SedimentDesorption}_{ij} \right) \frac{\text{PAtomicMass}}{\text{SedWaterRatio}_{ij}} \quad (12)$		
$(\mu\text{g P g}^{-1} \text{ time}^{-1})$		

Table 2-4 – General differential equations for suspended matter. The subscripts i and j refer to the line and columns of the model grid. These differential equations only describe changes due to non-conservative processes and provide the *sources-sinks* terms of Equation 1. The load terms refer to loads along the sea and river boundaries.

Total (TPM) and organic (POM) particulate matter (mg l^{-1})		
$\frac{d\text{TPM}_{ij}}{dt} = \text{TPMDep}_{ij} - \text{TPMResus}_{ij} + \text{PHYTONPP}_{ij} - \text{POMMiner}_{ij} + \text{TPMLoads}_{ij} \quad (13)$		
$\frac{d\text{POM}_{ij}}{dt} = \text{POMDep}_{ij} - \text{POMResus}_{ij} + \text{PHYTONPP}_{ij} - \text{POMMiner}_{ij} + \text{POMLoads}_{ij} \quad (14)$		
(following Duarte et al. (2003))		
TPMDep_{ij}	TPM Deposition rate	
TPMResus_{ij}	TPM Resuspension rate	
PHYTONPP_{ij}	Net Phytoplankton Production (in dry weight)	
TPMLoads_{ij}	TPM loads	$\text{mg l}^{-1} \text{ time}^{-1}$
POMDep_{ij}	POM Deposition rate	
POMResus_{ij}	POM Resuspension rate	
POMMiner_{ij}	POM mineralization	
POMLoads_{ij}	POM loads	
* - POM and POM fluxes are expressed in POM mass, Carbon, Nitrogen and Phosphorus units		

Phytoplankton ($\mu\text{g C l}^{-1}$)*

$$\frac{dPHY_{ij}}{dt} = PHY_{ij}(PHYGPP_{ij} - PHYExud_{ij} - PHYResp_{ij} - PHYMort_{ij}) - Gb_{ij}BIV_{ij}^{conv} + PHYLoads_{ij} \quad (15)$$

*For output, phytoplankton biomass is converted to Chlorophyll, assuming a Chlorophyll / Carbon ratio of 0.02 (Jørgensen et al., 1991)

$PHYGPP_{ij}$	Gross primary productivity	
$PHYExud_{ij}$	Exudation rate	
$PHYResp_{ij}$	Respiration rate	time^{-1}
$PHYMort_{ij}$	Mortality rate	
Gb_{ij}	Bivalve grazing rate	
BIV_{ij}^{conv}	Bivalve biomass converted to carbon	
$PHYLoads_{ij}$	Phytoplankton loads	$\mu\text{g C l}^{-1}\text{time}^{-1}$

Table 2-5 - General differential equations for benthic variables. The subscripts i and j refer to the line and columns of the model grid.

***Enteromorpha sp* (g DW m^{-2})**

$$\frac{dENT_{ij}}{dt} = ENT_{ij}(ENTGPP_{ij} - ENTResp_{ij} - ENTMort_{ij}) \quad (18)$$

$ENTGPP_{ij}$	Gross primary productivity	$\text{g DW m}^{-2} \text{time}^{-1}$
$ENTResp_{ij}$	Respiration rate	time^{-1}
$ENTMort_{ij}$	Mortality rate	time^{-1}

***Ulva sp.* (g DW m^{-2})**

$$\frac{dULV_{ij}}{dt} = ULV_{ij}(ULVGPP_{ij} - ULVResp_{ij} - ULVMort_{ij}) \quad (19)$$

$ULVGPP_{ij}$	Gross primary productivity	$\text{g DW m}^{-2} \text{time}^{-1}$
$ULVResp_{ij}$	Respiration rate	time^{-1}
$ULVMort_{ij}$	Mortality rate	time^{-1}

***Zostera noltii* (g DW m^{-2})**

Variables and equations as described in Plus et al. (2003)

***Ruditapes decussatus* (g DW m^{-2})**

$$\frac{dBIVB_{ij}}{dt} = BIVDens_{ij}(BIVAbsor_{ij} - BIVResp_{ij} - BIVExcr_{ij} - BIVMort_{ij}) \quad (20)$$

$$\frac{dBIVDens_{ij}}{dt} = -\mu BIVDens_{ij} + BIVSeed_{ij} - BIVHarv_{ij} \quad (21)$$

$BIVDens_{ij}$	Density	ind. m^{-2}
$BIVAbsor_{ij}$	Absorption rate	
$BIVResp_{ij}$	Respiration rate	$\text{g DW ind}^{-1} \text{time}^{-1}$
$BIVExcr_{ij}$	Excretion rate	
$BIVMort_{ij}$	Mortality rate	

$BIVSeed_{ij}$	Seeding rate	$g DW m^{-2} time^{-1}$
$BIVHarv_{ij}$	Harvest rate	
μ	Mortality rate	$time^{-1}$

Table 2-6 – Equations for suspended matter rate processes (see text).

TPM and POM

$$TPM_{Dep_{ij}} = SinkingVelocity_{ij} \frac{TPM_{ij}}{Depth_{ij}} \quad (22)$$

$$TPM_{Resus_{ij}} = Erate.VelocityShear_{ij} \quad (23)$$

if $\sqrt{Drag} |CurrentVelocity| < CritSpeed$ then
 $VelocityShear_{ij} = 0$ else

$$VelocityShear_{ij} = \min \left(\begin{array}{l} \frac{0.02^2}{(CritSpeed)^2} - 1.0, \\ \frac{(\sqrt{Drag} |CurrentVelocity|)^2}{(CritSpeed)^2} - 1.0 \end{array} \right) \quad (24)$$

0.02 – Threshold value to avoid very high resuspension rates (calibrated)

$$POM_{Dep_{ij}} = TPM_{Dep_{ij}} \frac{POM_{ij}}{TPM_{ij}} \quad (25)$$

$$POM_{Resus_{ij}} = TPM_{Resus_{ij}} \frac{POM_{ij}}{TPM_{ij}} \quad (26)$$

$$Drag = \frac{gn^2}{Depth^{1/3}} \text{ (calculated by the hydrodynamic object)} \quad (27)$$

n	Manning coefficient	
g	Gravity	$m s^{-2}$
$CritSpeed$	Velocity threshold for resuspension	$m s^{-1}$

Table 2-7 – Equations for phytoplankton rate processes. Each rate is multiplied by corresponding carbon, nitrogen or phosphorus stocks to obtain fluxes (see text).

Processes	Equations	Units
Vertically integrated (light limited productivity, from Steele's equation (Steele, 1962))	$P_g(I) = P_{max} \frac{\exp\left(\exp\left(-\frac{I_z}{I_{opt}}\right) - \exp\left(-\frac{I_0}{I_{opt}}\right)\right)}{kz} \quad (28)$ <p>where, <i>P_{max}</i> – Maximum rate of photosynthesis; <i>I_{opt}</i> – Optimal light intensity for photosynthesis; <i>I_z</i> – Light intensity at depth z;</p>	time ⁻¹
Light intensity at box depth	$I_z = I_0 \exp(-kz) \quad (29)$	μ E m ⁻² time ⁻¹
Light extinction coefficient	$k = 0.0243 + 0.0484TPM \quad (30)$ <p>(empirical relationship with TPM concentration used in Duarte et al. (2003))</p>	m ⁻¹
Light and temperature limited productivity	$P_g(I,T) = P_g(I)T_{limit} \quad (31)$ <p>where, <i>T_{limit}</i> – Temperature limitation factor</p>	time ⁻¹
Light, temperature and nutrient limited productivity	$PHYGPP_{ij} = P_g(I,T, Nut) = P_g(I,T) \min\left(\frac{N_{cell\ ij}}{k_{N_{cell}} + N_{cell\ ij}}, \frac{P_{cell\ ij}}{k_{P_{cell}} + P_{cell\ ij}}\right) \quad (32)$ <p>where, <i>K_{N_{cell}}</i> – Half saturation constant for growth limited by nitrogen cell quota; <i>K_{P_{cell}}</i> – Half saturation constant for growth limited by phosphorus cell quota.</p>	time ⁻¹
Nitrogen cell quota	$N_{cell\ ij} = \frac{PHYN_{ij}}{PHYC_{ij}} \quad (33)$ <p>where, <i>PHYN_{ij}</i> and <i>PHYC_{ij}</i> represent phytoplankton biomass in nitrogen and carbon units, respectively</p>	mg N mg C ⁻¹
Phosphorus cell quota	$P_{cell\ ij} = \frac{PHYP_{ij}}{PHYC_{ij}} \quad (34)$ <p>where, <i>PHYP_{ij}</i> represent phytoplankton biomass in phosphorus units</p>	mg P mg C ⁻¹
Nitrogen uptake	$PHYUptakeN_{ij} = V_N \cdot PHYN_{ij} \quad (35)$	μg N L ⁻¹ time ⁻¹
Phosphorus uptake	$PHYUptakeP_{ij} = V_P \cdot PHYP_{ij} \quad (36)$	μg P L ⁻¹ time ⁻¹

<p>Nitrogen uptake rate (VN)</p>	<p>If $N_{min} < PHYN_{ij} < N_{max}$ and $PHYN_{ij} / PHYP_{ij} < maxN/P_{ij}$</p> $V_{Ammonium} = V_{maxN} \frac{NH_{4ij}}{k_{Ammonium} + NH_{4ij}} \left(1 - \frac{N_{cellij}}{N_{max}} \right) \quad (37)$ $V_{Nitrate + Nitrite} = \max \left(0, V_{maxN} - V_{Ammonium} \right) \cdot \frac{NO_{ij}}{k_{Nitrate+Nitrite} + NO_{ij}} \left(1 - \frac{N_{cellij}}{N_{max}} \right) \quad (38)$ $V_N = V_{Ammonium} + V_{Nitrate + Nitrite}$ <p>else $V_N = 0, \quad (39)$ where</p> <p>N_{min} – minimal nitrogen cell quota (mg N mg C⁻¹); N_{max} - maximal nitrogen cell quota (mg N mg C⁻¹); $K_{Ammonium}$ – half saturation constant for ammonium uptake (μmol N L⁻¹); $maxN/P_{ij}$ – Maximal cellular nitrogen:phosphorus ratio; V_{maxN}– Maximal uptake rate (d⁻¹); $K_{Nitrate+Nitrite}$ – half saturation constant for Nitrate + Nitrite uptake (μmol N L⁻¹);</p>	<p>time⁻¹</p>
<p>Phosphorus uptake rate (VP)</p>	<p>If $PHOS_{min} < PHYP_{ij} < PHOS_{max}$ and $PHYN_{ij} / PHYP_{ij} > minN/P_{ij}$</p> $V_P = V_{maxP} \frac{PO_{4ij}}{k_P + PO_{4ij}} \left(1 - \frac{P_{cellij}}{PHOS_{max}} \right) \quad (40)$ <p>else $VP = 0,$ where</p> <p>$PHOS_{min}$ – minimal phosphous cell quota (mg P mg C⁻¹); $PHOS_{max}$ - maximal phosphous cell quota (mg P mg C⁻¹); K_p – half saturation constant for phosphous uptake (μmol P L⁻¹); $minN/P_{ij}$ – Minimal cellular nitrogen:phosphorus ratio; V_{maxP}– Maximal uptake rate (d⁻¹);</p>	<p>time⁻¹</p>
<p>Phytoplankton exudation rate of Carbon</p>	$PHYExud_{ij} = Exud \cdot PHYGPP_{ij}, \text{ where } (41)$ <p>$Exud$ – Fraction exudated;</p>	<p>time⁻¹</p>
	$PHYResp_{ij} = \left(R_0 + R_{dark} \cdot Tlimit \cdot \overline{DailyMeanGPP_{ij}} \right) \cdot \frac{CarbonToOxygen}{ChlorophyllToCarbon} \cdot OxygenMolecularWeight \cdot 24 \quad (42)$ <p>during the night</p> $PHYResp_{ij} = \left(R_0 + R_{dark} \cdot Tlimit \cdot DLratio \cdot \overline{DailyMeanGPP_{ij}} \right) \cdot \frac{CarbonToOxygen}{ChlorophyllToCarbon} \cdot OxygenMolecularWeight \cdot 24$	

Phytoplankton respiration rate	<p>(43)</p> <p>during the day, where</p> <p>R_0 – Maintenance respiration ($\text{mmol O}_2 \text{ mg Chl}^{-1} \text{ h}^{-1}$);</p> <p>$R_{dark}$ – Linear coefficient of increase in biomass-specific dark respiration with gross photosynthesis (dimensionless);</p> <p>DLratio – Ratio between respiration in the light and respiration in the dark (dimensionless);</p> <p>$\overline{\text{DailyMeanGPP}_{ij}}$ - Daily integrated gross productivity ($\text{mmol O}_2 \text{ mg Chl}^{-1} \text{ h}^{-1}$);</p> <p>CarbonToOxygen – Conversion factor between oxygen consumed and carbon produced in respiration (mg C mg O_2^{-1});</p> <p>ChlorophyllToCarbon – Conversion factor from chlorophyll to carbon (mg C mg Chl^{-1})</p>	time^{-1}
Temperature limitation factor	<p>$T_{limit} = \exp\left(\text{TempAugRate}\left(T_{ij} - T_0\right)\right)$ (44)</p> <p>where,</p> <p>TempAugRate – Temperature augmentation rate;</p> <p>T_0 – Reference temperature.</p>	dimensionless
Nitrogen mortality loss	$PHYMortN_{ij} = PHYMort_{ij} \cdot PHYC_{ij} \cdot N_{cell_{ij}}$ (45)	$\mu\text{g N l}^{-1}\text{time}^{-1}$
Phosphorus mortality loss	$PHYMortP_{ij} = PHYMort_{ij} \cdot PHYC_{ij} \cdot P_{cell_{ij}}$ (46)	$\mu\text{g P l}^{-1}\text{time}^{-1}$
Carbon settling loss rate	<p>$PHYSet_{ij} = \frac{\text{SettlingSpeed}}{\text{Depth}_{ij}}$, (47)</p> <p>where,</p> <p>SettlingSpeed – Fall velocity of phytoplankton cells (m d^{-1});</p> <p>Depth_{ij} – Depth of layer j in column i (m)</p>	time^{-1}
Nitrogen settling loss	$PHYSetN_{ij} = \text{SettlingSpeed} \cdot \frac{PHYN_{ij}}{\text{Depth}_{ij}}$ (48)	$\mu\text{g N l}^{-1}\text{time}^{-1}$
Phosphorus settling loss	$PHYSetP_{ij} = \text{SettlingSpeed} \cdot \frac{PHYP_{ij}}{\text{Depth}_{ij}}$ (49)	$\mu\text{g P l}^{-1}\text{time}^{-1}$

Table 2-8 – Equations for *Enteromorpha sp.* and *Ulva sp.* rate processes. Each rate is multiplied by corresponding dry weight, carbon, nitrogen or phosphorus stocks to obtain fluxes (see text).

Processes	Equations	Units
Steele's equation (Steele, 1962))	$P_g(I) = P_{max} \frac{I_z}{I_{opt}} \exp\left(1 - \frac{I_z}{I_{opt}}\right) \quad (50)$ <p>where, <i>P_{max}</i> – Maximum rate of photosynthesis; <i>I_{opt}</i> – Optimal light intensity for photosynthesis; <i>I_z</i> – Light intensity at depth z;</p>	time ⁻¹
Light and temperature limited productivity	$P_g(I,T) = P_g(I) \cdot T_{limit} \quad (51)$ <p>where, <i>T_{limit}</i> – Temperature limitation factor</p>	time ⁻¹
Temperature limitation factor	$T_{limit} = \frac{1}{1 + \exp(-TempCoeff (T_{ij} - T_0))} \quad (52)$ <p>where, TempCoeff – Temperature coefficient; <i>T₀</i> – Reference temperature.</p>	dimensionless
Light, temperature and nutrient limited productivity	$ENTGPP_{ij} \text{ or } ULVGPP_{ij} = P_g(I,T, Nut) = P_g(I,T) \min\left(\frac{N_{cellij} - N_{min}}{N_{max} - N_{min}}, \frac{P_{cellij} - PHOS_{min}}{PHOS_{max} - PHOS_{min}}\right) \quad (53)$ <p>Symbols as before for phytoplankton (cf. – Table 7)</p>	time ⁻¹
<i>Enteromorpha</i> nitrogen uptake	$EntUpDIN_{ij} = V_N \cdot ENT_{ij} \quad (54)$	g N m ⁻² time ⁻¹
<i>Enteromorpha</i> phosphorus uptake	$EntUpDIN_{ij} = V_P \cdot ENT_{ij} \quad (55)$	g P m ⁻² time ⁻¹
<i>Ulva</i> nitrogen uptake	$UlvUpDIN_{ij} = V_N \cdot ULV_{ij} \quad (56)$	g N m ⁻² time ⁻¹
<i>Ulva</i> phosphorus uptake	$UlvUpDIN_{ij} = V_P \cdot ULV_{ij} \quad (57)$	g P m ⁻² time ⁻¹

<p>Nitrogen uptake rate (V_N)</p>	$V_N = V_{\max N} \frac{NH_{4ij} + NO_{ij}}{k_{DIN} + NH_{4ij} + NO_{ij}} \max \left(\frac{N_{\max} - N_{cellij}}{N_{\max} - N_{min}}, 0 \right)$ <p>(58)</p> <p>where k_{DIN} – half saturation constant for inorganic nitrogen uptake ($\mu\text{mol N L}^{-1}$);</p>	<p>time⁻¹</p>
<p>Phosphorus uptake rate (V_P)</p>	$V_P = V_{\max P} \frac{PO_{4ij}}{k_P + PO_{4ij}} \max \left(\frac{PHOS_{\max} - P_{cellij}}{PHOS_{\max} - PHOS_{min}}, 0 \right)$ <p>(59)</p>	<p>time⁻¹</p>
<p><i>Enteromorpha</i> mortality rate</p>	$ENT_{Mortij} = ENT_{DeathLoss} \cdot ENT_{ij}^{\beta} + K_{TEnt} \cdot \frac{\max(OxygenDemand_{ij} - DO_{ij}, 0)}{OxygenDemand_{ij}} \cdot ENT_{ij}$ <p>K_{TEnt} – Mortality coefficient for oxygen limitation $OxygenDemand_{ij}$ – Quantity of oxygen necessary over one time step to support <i>Enteromorpha</i> respiration (only positive when respiration > photosynthesis)</p> <p>(60)</p>	<p>time⁻¹</p>
<p><i>Ulva</i> mortality rate</p>	$ULV_{Mortij} = ULV_{DeathLoss} \cdot ULV_{ij}^{\beta} + K_{TUlva} \cdot \frac{\max(OxygenDemand_{ij} - DO_{ij}, 0)}{OxygenDemand_{ij}} \cdot ULV_{ij}$ <p>K_{TEnt} – Mortality coefficient for oxygen limitation $OxygenDemand_{ij}$ – Quantity of oxygen necessary over one time step to support <i>Ulva</i> respiration (only positive when respiration > photosynthesis)</p> <p>(61)</p>	<p>time⁻¹</p>

Table 2-9 - Equations for *Ruditapes decussatus* rate processes.

Processes	Equations	Units
Clearance rate	$CR = aW^{FC} \quad (62)$ <p>Where, a – allometric parameter; W – meat dry weight (g); FC – allometric exponent for clearance</p>	L individual ⁻¹ day ⁻¹
Coefficient	$a = \frac{CR_{st}}{W_{st}^{FC}} \quad (63)$ <p>Where, CR_{st} – Clearance rate of a standard animal; W_{st} – meat dry weight of a standar clam (g)</p>	
Clearance rate of a standard clam	$CR_{st} = (-0.003TPM_{ij} + 1.426) f(T) f(DO) \quad (64)$	L individual ⁻¹ day ⁻¹
Temperature limitation	<p><i>if</i> $T_{ij} < 20^{\circ}C$</p> $f(T) = 1.0 + 0.045(T_{ij} - 20.0) \quad (65)$ <p><i>else</i></p> $f(T) = 1.0 - 0.040(T_{ij} - 20.0) \quad (66)$	Dimensionless
Dissolved oxygen limitation	<p><i>if</i> $DO_{satij} > 28\%$</p> $f(DO) = 1 \quad (67)$ <p><i>else</i></p> $f(DO) = 1.0 + 0.06(DO_{satij} - 28.0)$	Dimensionless
Suspended matter filtration	$Cons = CR.TPM_{ij}$	g individual ⁻¹ day ⁻¹
Pseudofaeces production rate	$\delta = ThresCons - Cons$ $PF = PFmax(1 - \exp(-xkp.\delta)) \quad (68) \text{ where,} \quad (69)$ <p>$ThresCons$ – Threshold filtration rate; $PFmax$ – Pseudofaeces maximal production rate; xkp – Coefficient</p>	Dimensionless
Suspended matter ingestion	$Ing = Cons(1 - PF)conv \quad (70)$	g individual ⁻¹ day ⁻¹
Absorption	$A = Ing.AE \quad (71)$ <p>Where, AE – Absorption efficiency</p>	J individual ⁻¹ day ⁻¹ (it is converted to/from g individual ⁻¹ day ⁻¹ assuming an energy contents for the clams of 20000 J g ⁻¹ (Sobral, (1995))
Absorption efficiency	$AE = AEmax - \frac{AP}{OCI}$	Dimensionless

	Where, <i>AEmax</i> – Maximum absorption efficiency; <i>AP</i> – Empirical coefficient; <i>OCI</i> – Organic contents of ingested food	
Respiration rate	$R = R_{st} \left(\frac{W}{W_{st}} \right)^{RC} \quad (72) \text{ where,}$ <p><i>R_{st}</i> – respiration of a standar mussel (1 g DW); <i>RC</i> – respiration exponent</p>	<p>J individual⁻¹ day⁻¹ (it is converted to/from g individual⁻¹ day⁻¹ assuming an energy contents for the clams of 20000 J g⁻¹ (Sobral, 1995))</p>
Respiration rate of a standard mussel	<i>If DO_{sat}_{ij} < 28% R_{st} = 1.5 else R_{st} = 3.1</i>	J day ⁻¹ ind ⁻¹

Table 2-10 – Model parameters and respective values. Most values were calibrated from ranges reported by quoted authors.

Object	Parameter	Value	Reference
Hydrodynamic 2D object	Manning coefficient	0.03 s m ^{-1/3}	Grant and Bacher (2001)
	Eddy diffusivity	5 m ² s ⁻¹	Neves (1985)
Suspended matter object	<i>CritSpeed</i>	0.00773 m s ⁻¹	Calibrated
	<i>SinkingVelocity</i>	0.4 and 20 m day ⁻¹ for POM and TPM, respectively	Calibrated
	<i>Erate</i>	432 g m ⁻² day ⁻¹	Calibrated
Phytoplankton object	<i>Nmin</i>	0.1 mg N mg C ⁻¹	Jørgensen et al (1991)
	<i>Nmax</i>	0.53 mg N mg C ⁻¹	“
	<i>KAmmonium</i>	2.94 μmol N l ⁻¹	“
	<i>maxN/P_{ij}</i>	291	“
	<i>V_{maxP} and V_{maxN}</i>	1.08 d ⁻¹	Cochlan & Harrison (1991)
	<i>KNitrate+Nitrite</i>	30 μmol N l ⁻¹	Jørgensen et al (1991)
	<i>PHOSmin</i>	0.002 mg P mg C ⁻¹	“
	<i>PHOSmax</i>	0.08 mg P mg C ⁻¹	“
	<i>minN/P_{ij}</i>	4	“
	<i>Kp</i>	2 μmol P l ⁻¹	“
	<i>P_{max}</i>	1.1 d ⁻¹	“
	<i>I_{opt}</i>	850 μE m ⁻² s ⁻¹	“
	<i>K_{Ncell}</i>	0.028 mg N mg C ⁻¹	Calibrated
	<i>K_{Pcell}</i>	0.004 mg P mg C ⁻¹	Calibrated
	<i>Exud</i>	0.1	Jørgensen et al (1991)
	<i>R₀</i>	0.02 mmol O ₂ mg Chl ⁻¹ 1 h ⁻¹	Langdon (1993)
	<i>R_{dark}</i>	0.3	Calibrated
	<i>DLratio</i>	2	Langdon (1993)
	CarbonToOxygen	0.3125 mg C mg O ₂ ⁻¹	Vollenweider (1974)
	ChlorophyllToCarbon	50 mg C mg Chl ⁻¹	Jørgensen & Jørgensen (1991)
	<i>TempAugRate</i>	0.069 °C ⁻¹	Estimated
	<i>T₀</i>	0°C for photosynthesis and 25°C for respiration	Calibrated
	<i>SettlingSpeed</i>	1 m d ⁻¹	Mann & Lazier (1996)
<i>PHYMort_{ij}</i>	0.05 day ⁻¹	Jørgensen & Jørgensen (1991)	
<i>Enteromorpha sp</i>	<i>P_{max}</i>	6.93 mg C g(DW)-1 h-1	Serpa (2004)
	<i>I_{opt}</i>	335 μE m ⁻² s ⁻¹	“
	<i>ENTResp_{ij}</i>	0.04 mg C g(DW)-1 h-1	“
	<i>T₀</i>	0°C	“
	<i>TempCoeff</i>	1°C	“
	<i>Nmin</i>	0.01 gN g(DW)-1	“
	<i>Nmax</i>	0.035 gN g(DW)-1	“

	<i>PHOSmin</i>	5 X 10 ⁻⁴ gP g(DW) ⁻¹	“
	<i>PHOSmax</i>	4 X 10 ⁻³ gP g(DW) ⁻¹	“
	<i>V_{maxN}</i>	1.68 mg N g(DW) ⁻¹ h ⁻¹	“
	<i>V_{maxP}</i>	0.23 mg P g(DW) ⁻¹ h ⁻¹	“
	<i>KDIN</i>	0.25 mg L ⁻¹	“
	<i>Kp</i>	0.025 mg L ⁻¹	“
	<i>ENTDeathLoss</i>	0.00125 h ⁻¹	“
	<i>Beta</i>	0.84	Solidoro et al. (1997)
	<i>KTEnt</i>	1	Calibration
<i>Ulva sp.</i>	<i>P_{max}</i>	5.14 mg C g(DW) ⁻¹ h ⁻¹	Serpa (2004)
	<i>I_{opt}</i>	358 μE m ⁻² s ⁻¹	“
	<i>ULVResp_{ij}</i>	0.25 mg C g(DW) ⁻¹ h ⁻¹	“
	<i>T₀</i>	0°C	“
	<i>TempCoeff</i>	1°C	“
	<i>N_{min}</i>	0.01 gN g(DW) ⁻¹	“
	<i>N_{max}</i>	0.04 gN g(DW) ⁻¹	“
	<i>PHOSmin</i>	6 X 10 ⁻⁴ gP g(DW) ⁻¹	“
	<i>PHOSmax</i>	3.9 X 10 ⁻³ gP g(DW) ⁻¹	“
	<i>V_{maxN}</i>	1 mg N g(DW) ⁻¹ h ⁻¹	“
	<i>V_{maxP}</i>	0.3 mg P g(DW) ⁻¹ h ⁻¹	“
	<i>KDIN</i>	0.25 mg L ⁻¹	“
	<i>Kp</i>	0.025 mg L ⁻¹	“
	<i>ULVDeathLoss</i>	0.00125 h ⁻¹	“
	<i>beta</i>	0.84	Solidoro et al. (1997)
	<i>KTUlva</i>	1	“
<i>Zostera noltii</i> (refer Plus et al. (2003) for parameter meaning)	<i>ϑ_{pmax}</i>	8X10 ⁻⁴ g O ₂ mmol C ⁻¹ °C ⁻¹ day ⁻¹	
	<i>P_{max}^{0°C}</i>	0.0 g O ₂ mmol C ⁻¹ day ⁻¹	
	<i>I_{kmax}</i>	100 Wm ⁻²	Calibration
	<i>I_{kmin}</i>	35 Wm ⁻²	
	<i>ϑ_{LR}</i>	4.5X10 ⁻⁵ g O ₂ mmol C ⁻¹ °C ⁻¹ day ⁻¹	
	<i>LR_{0°C}</i>	5.9X10 ⁻⁴ g O ₂ mmol C ⁻¹ day ⁻¹	
<i>Ruditapes decussatus</i>	<i>W_{st}</i>	0.3 g	Sobral (1995)
	<i>FC</i>	0.7	“
	<i>ThresCons</i>	0.0 g individual ⁻¹ day ⁻¹	Calibration
	<i>xkp</i>	0.8	“
	<i>PFmax</i>	1.0	“
	<i>AP</i>	0.07	“
	<i>AEmax</i>	0.85	“
	<i>μ</i>	4X10 ⁻³ day ⁻¹	Falcão et al. (2000)

2.2.1. Hydrodynamic object

The hydrodynamic object was described in a previous report (Duarte et al., 2005). This object allows the output of time integrated current velocities and flow values for each grid cell. These outputs may later be used to run the remaining objects without the necessary calculation overhead of the hydrodynamic processes. Therefore, a specific transport object was implemented in EcoDynamo just to handle the time series calculated by the hydrodynamic object. This transport object computes the equation of continuity, as described in Duarte et al. (2005) and the transport equation (1) for all pelagic variables of the other objects.

2.2.2. Wind object

This object returns wind speed forcing variable average values to the water temperature object. These values are then used to calculate water heat losses through evaporation.

2.2.3. Air temperature object

This object reads forcing variable air temperature values and returns them to the water temperature object, to be used to calculate sensible heat exchanges between the water and the atmosphere.

2.2.4. Light intensity and water temperature objects

Light intensity and water temperature were calculated by a light and a water temperature object using standard formulations described in Brock (1981) and Portela & Neves (1994). Submarine light intensity was computed from the Lambert-Beer law. The water light extinction coefficient was computed by the suspended matter object (cf. – 2.2.6).

2.2.5 Dissolved substances object

The concentrations of dissolved inorganic nitrogen (DIN) - ammonium, nitrite and nitrate -, inorganic phosphorus and oxygen in each of the model grid cells are calculated

as a function of biogeochemical and transport processes, including exchanges with the sea, loads from rivers and waste water treatment plants (WTPs), and exchanges across the sediment water interface (Figs. 2-1, 2-2 and Table 2-2).

These variables are also calculated in pore water (Table 2-3). Both the nitrogen and phosphorus cycles are simulated using equations and parameters described in Chapelle (1995). The only exception is the reaeration coefficient, calculated as a function of wind speed, following Burns (2000). Phytoplankton and macroalgae remove nutrients from flowing water. *Zostera noltii* also removes nutrients from pore water through the roots (Plus et al., 2003).

2.2.6 Suspended matter object

This object computes total particulate matter (TPM in mg L^{-1}) and particulate organic matter (POM in mg L^{-1}) from deposition and resuspension rates, from the exchanges with the sea and with other boxes (transport by the hydrodynamic object), and from the net contribution of phytoplankton biomass (Figs. 2-1, 2-2 and Table 2-4). POM mineralization is calculated as in Chapelle (1995), returning the resulting inorganic nitrogen and phosphorus to the dissolved substances object.

Deposition of TPM in each grid cell is based on sinking velocity and cell depth (returned by the hydrodynamic object). Sinking velocity is considered constant but with different values for inorganic and organic matter (calibrated) (Tables 2-4, 2-6 and 2-10).

Resuspension of TPM in each grid cell is calculated as a function of current velocity and bottom drag, returned by the hydrodynamic object (Table 2-6). Below a critical velocity value, resuspension does not occur. Above a certain threshold for the product of bottom drag times current velocity (velocity shear), resuspension is assumed constant. This is to avoid unrealistically high resuspension rates. This object is partly based on a Stella model developed by Grant and Bacher (unpublished).

The light extinction coefficient (m^{-1}) is calculated from an empirical relationship with TPM (Equation 30 in Table 2-7), obtained from historical data for Sungo Bay (Bacher, pers com).

2.2.7 Phytoplankton object

Phytoplankton productivity is described as a function of light intensity (depth integrated Steele's equation) (Steele, 1962), temperature and a limiting nutrient – nitrogen or phosphorus (Tables 2-4 and 2-7). In this model, phytoplankton is represented through chlorophyll, carbon, nitrogen and phosphorus pools. This allows the necessary bookkeeping calculations on cell quotas. Traditional approaches with models based solely on nitrogen or phosphorus do not allow these computations. Internal cell quotas are then used to limit carbon fixation through photosynthesis. A nutrient limiting factor in the range 0 – 1 is calculated both for internal nitrogen and phosphorus. The lowest obtained value is then multiplied by light and temperature limited photosynthesis following Liebig's law of minimum.

Nutrient uptake and limitation is described as a three-stage process (Table 2-7, equations 35-40), following Jørgensen & Bendoricchio (2001) :

- (i) The uptake of nitrogen and phosphorus is dependent on their concentration in the water, on their cell quotas and on the ranges of their cellular ratios;
- (ii) After uptake, nutrients accumulate in the cells;
- (iii) Internal nutrient concentration is used to limit phytoplankton productivity.

A Michaelis-Menten equation is used to relate nutrient uptake with their concentration in the water, following several authors (e.g. Parsons et al., 1984; Ducobu et al., 1998; Jørgensen & Bendoricchio, 2001). The parameters of this equation are the half-saturation constant and the maximum uptake rate. These were taken from the literature, within the range of measured values (Cochlan and Harrison, 1991; Jørgensen et al., 1991). The Michaelis-Menten equation is not the only regulating mechanism of nutrient uptake, which is also constrained by current cell quotas to avoid values outside ranges reported in the literature. When N:P ratios are outside limits currently measured, N or P uptake is constrained. Nitrogen uptake rate is calculated first for ammonium nitrogen and then for nitrite + nitrate, reducing their uptake proportionally to ammonium uptake. This is based on the usual assumption that ammonium is the preferred nitrogen source

for phytoplankton (Parsons et al., 1984). Phytoplankton respiration is based on the model of Langdon (1993) (Table 2-7, equations 42 and 43).

2.2.8 *Enteromorpha* spp. and *Ulva* spp. objects

These objects were computed as described in Solidoro et al. (1997) and Serpa (2004) (Tables 2-5 and 2-8).

2.2.9 *Zostera noltii* object

This object computes *Z. noltii* photosynthesis, respiration, nutrient uptake, translocation and reclamation, growth, mortality and recruitment as described in Plus et al. (2003), except for some modifications described below. In Plus et al. (2003), growth is calculated without considering any limit to plant individual weight or size. Therefore, the model may produce biomass standing stocks and plant densities that imply unrealistically large individual sizes. This can be avoided by careful calibration. However, in the present model it was decided to create some mechanisms to avoid this potential problem. This was done by defining an asymptotic individual weight for *Zostera* leaves. Any biomass production leading to growth above that asymptotic value is released as detritus to the suspended matter object. *Z. noltii* parameters differing from those reported in Plus et al. (2003) are listed in Table 2-10, using the same symbols of those authors.

2.2.10 *Ruditapes decussatus* object

Differential and rate equations for the clam object are depicted in Tables 2-5 and 2-9, respectively. Parameters are listed in Table 2-10. Rate equations were obtained from ecophysiology data reported in Sobral (1995). The general approach to simulate bivalve feeding and growth is similar to other works (e.g. Raillard et al., 1993; Raillard & Ménesguen, 1994; Ferreira et al., 1998; Duarte et al., 2003). Clearance rate is computed from an empirical relationship with TPM, water temperature and oxygen concentration. Temperature limitation is calculated from a direct linear relationship with water temperature, until 20°C, and an inverse linear relationship, above that value. Oxygen

limitation is calculated as a linear function of oxygen saturation, when this is below 28% saturation (hypoxia conditions). Ingestion is calculated from clearance and pseudofaeces production rate. Absorption is calculated from ingestion and faeces production and the usual asymptotic relationship with ingested organics (e.g. Hawkins et al., 1998). Scope for growth is calculated from absorption and metabolism. Respiration is calculated as a function of oxygen saturation. When saturation is below 33 %, respiration rate decreases (Sobral, 1995). Allometric relationships are used to correct for bivalve weight.

2.3 Model setup

In what concerns pelagic variables, the model was initialized with the same concentrations over all model domain, under the assumption that local and exchange processes would produce a rapid change (within a few hours) of initial conditions, which was the case. Regarding pore water and sediment variables, uniform values were used to initialize conditions in similar sediment types. These were defined as sand, sand-muddy, muddy-sand and muddy. Water, pore water and sediment variable values were obtained from a database available at the DITTY project web site (www.dittyproject.org). Sediment types and distribution of benthic variables were obtained from a GIS developed partly during the DITTY project (Rodrigues et al., 2005). Figs 2-4 – 2-6 summarize distribution of sediment types and benthic variables.

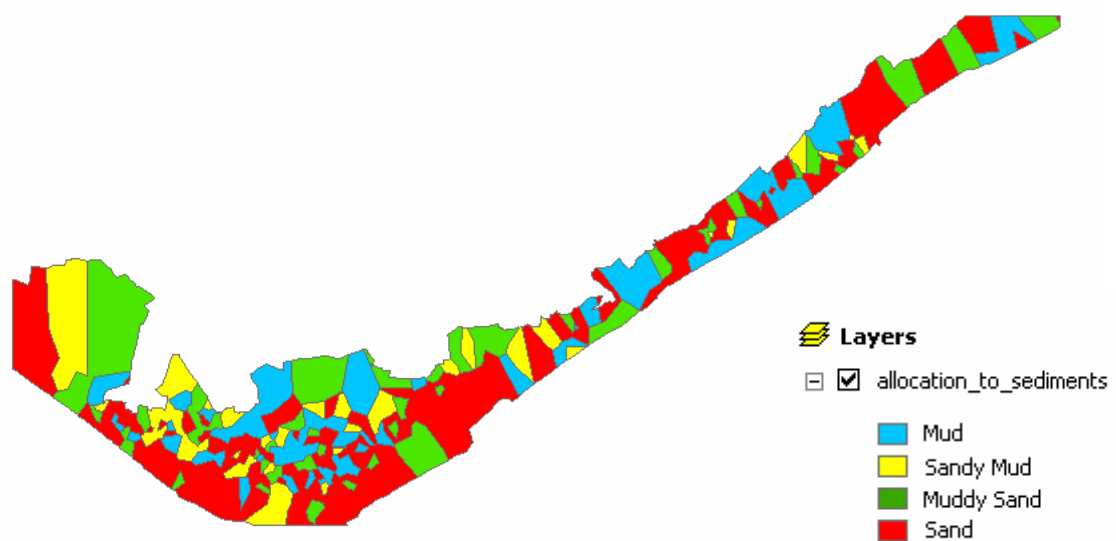


Fig. 2-4 – GIS image showing sediments type distribution in Ria Formosa.

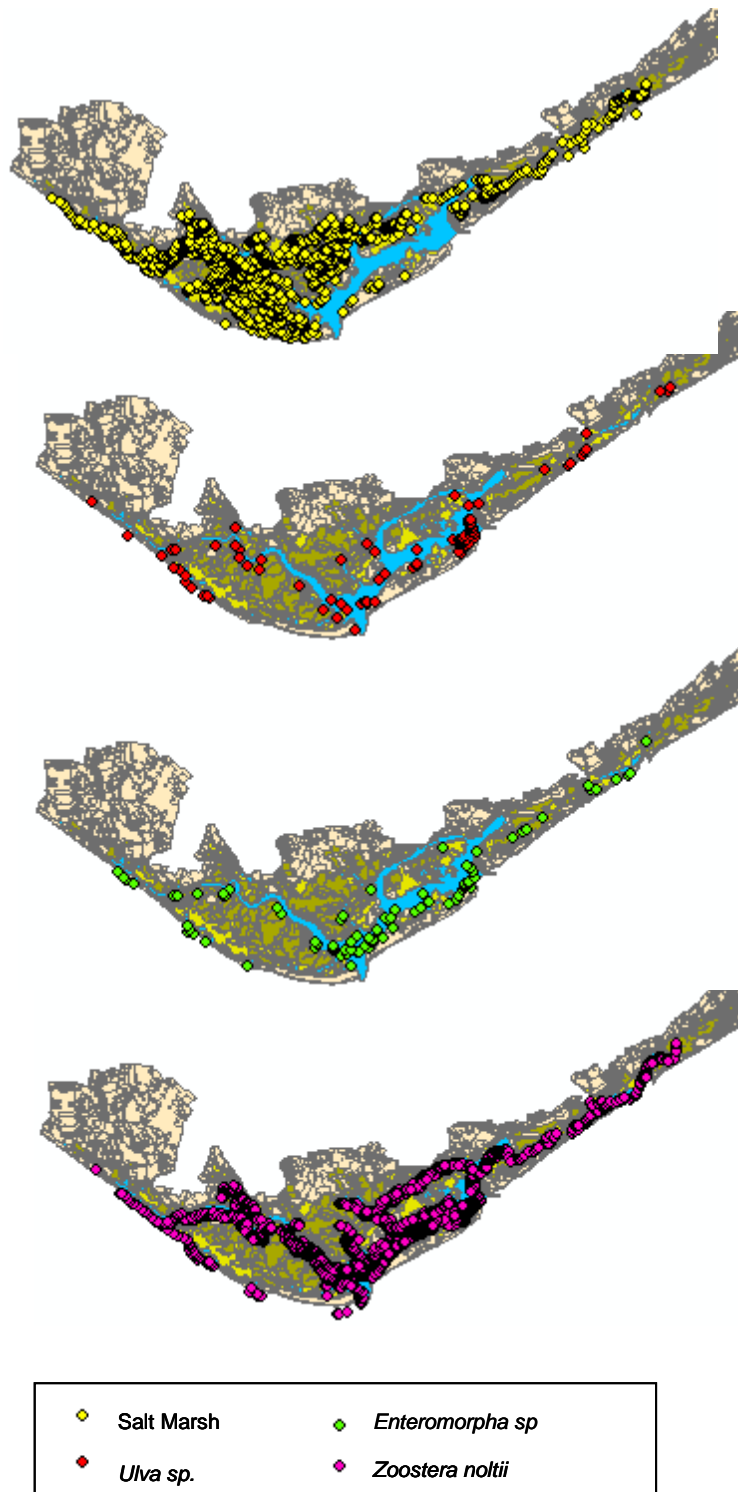


Fig. 2-5 – GIS images showing Ria Formosa benthic species considered in this work – Salt Marshes, *Ulva sp.*, *Enteromorpha sp.* and *Zoostera noltii*.

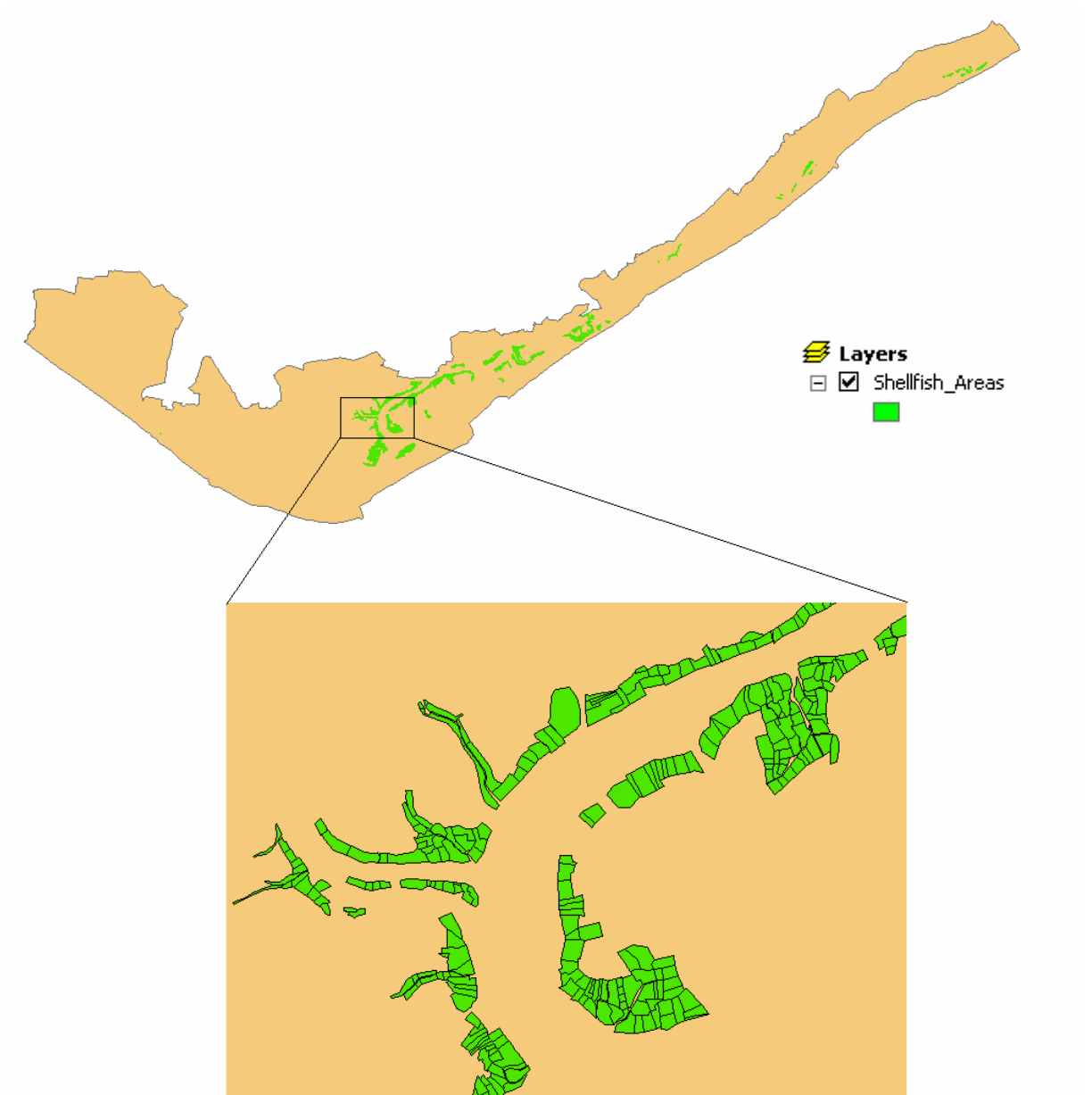


Fig. 2-6 – Ria Formosa shellfish farming areas.

2.4 Model testing

Validation of the hydrodynamic sub-model was carried out before (Duarte et al., 2005; Duarte et al, submitted) and will not be discussed in this work. The same applies to the SWAT model application used to force the lagoon model at river boundaries (Guerreiro & Martins, 2005).

Regarding the biogeochemical sub-model, a significant part of model parameters was taken from the literature: e.g. water column and sediment biogeochemistry, seagrass, macroalgal and some phytoplankton parameters from Chapelle (1995), Solidoro et al. (1997), Plus et al. (2003), Serpa (2004) and Falcão (1996), respectively. Some parameters were calibrated with a zero dimensional (0D) version of the model. Several simulations were carried out with full model complexity to check if predictions remained within reasonable limits.

For the purposes of model calibration and validation it is important to have data on boundary and forcing conditions collected simultaneously with data inside the lagoon. Most of the data available for Ria Formosa does not fulfil these requirements – for some years there is data collected inside the lagoon but not at the sea and river boundaries and vice-versa. Fortunately, there is a relatively old data set for 1992 (Falcão, 1996) that includes nutrient data inside and outside (at the sea boundary) the lagoon sampled at a number of stations depicted in Fig 2-3. This data set was used to test the model. This test simulation will be hereafter referred as the “standard simulation”. However, given the fact that lagoon bathymetry changes very rapidly and that the bathymetry used in the model was obtained in a relatively recent survey (conducted by the Portuguese Hydrographic Institute in 2000), the comparison between observed and predicted data should be carried out with caution.

3 Results and discussion

Comparisons between observed and predicted values in the Standard simulation (cf. – Methodology – Model testing) are shown in Figs. 3-1 to 3-6 for nitrate, ammonia, phosphate and water temperature. Observations were made during the ebb and during the flood for each sampling occasion. Nutrient flood values are lower than ebb values and closer to the sea boundary conditions, except for nitrate in some occasions. This is also the case for simulated data, as can be seen for nitrate in Fig. 3-1, shown together with water depth. The small number of observations prevents any powerful statistical test to quantify model performance. Furthermore, data is available only for a small number of stations located not very distant from one another (c.a. 500 – 1000 m) and for a small number of variables. However, in most situations, the ranges predicted by the model are within those observed, with the poorer performance for ammonia - overestimated by the model.

Fig. 3-7 shows an example of two contour plots – for nitrate and chlorophyll. The range for nitrate is very large (up to $880 \mu\text{mol L}^{-1}$) as a result of river inputs. Apart from river mouths, concentrations are usually around $1 \mu\text{mol L}^{-1}$.

Comparisons between model predictions and ranges reported in several works were also made for the biomass of benthic species, water column chlorophyll, sediment pore water nutrient and oxygen concentrations and sediment carbon, nitrogen and phosphorus contents. However, available data for these variables were obtained in different years than water quality data shown in Figs. 3-1 – 3-6. Therefore, comparisons with results reported in other authors (Aníbal, 1998; Falcão et al., 2000; Santos et al., 2000) were just to make sure that model predictions remained within reasonable limits, which was the case.

Figs. 3-8 – 3-10 show predicted average *Z. noltii*, *Enteromorpha* sp., *Ulva* sp. biomasses and chlorophyll concentrations over a period of one year. The model may underestimate *Z. noltii* biomass, which has been reported to reach values in excess of $200 \text{ g (DW) m}^{-2}$ in some areas, without a very clear seasonal pattern (Santos et al., 2000). However, considering that the results shown in Fig. 3-8 are averages over all habitat area (cf. –

Fig. 2-5), this underestimation is probably not very large. In what concerns macroalgae, *Enteromorpha* and *Ulva* biomasses hardly reach 50 and 10 g (DW) m⁻², respectively, with the latter being usually below 5 g (DW) m⁻² (Aníbal, 1998). Fig 3-11 shows *R. decussatus* average individual weight for the same period. Clam growth is similar to growth curves reported in previous works (Falcão et al., 2000).

Table 3-1 synthesis average values predicted by the model for a period of one year for several sediment and pore water variables, considering the sediment types depicted in Fig. 2-4. All values are well within ranges measured in Ria Formosa at the different sediment types as checked in a database available at the DITTY web site.

Although presented results do not allow a complete and systematic testing of the model in the light of available data, due to the lack of a complete dataset for one year, including boundary conditions, the model, as it is, seems to be a good starting point as a management tool. Further testing is necessary and also several improvements in the definition of initial conditions. For example, GIS data presented in Fig. 2-5 are only an approximate representation of the distribution of macroalgae and seagrasses. Furthermore, the functional role of salt marshes in Ria Formosa need to be accessed to improve their forcing to the model.

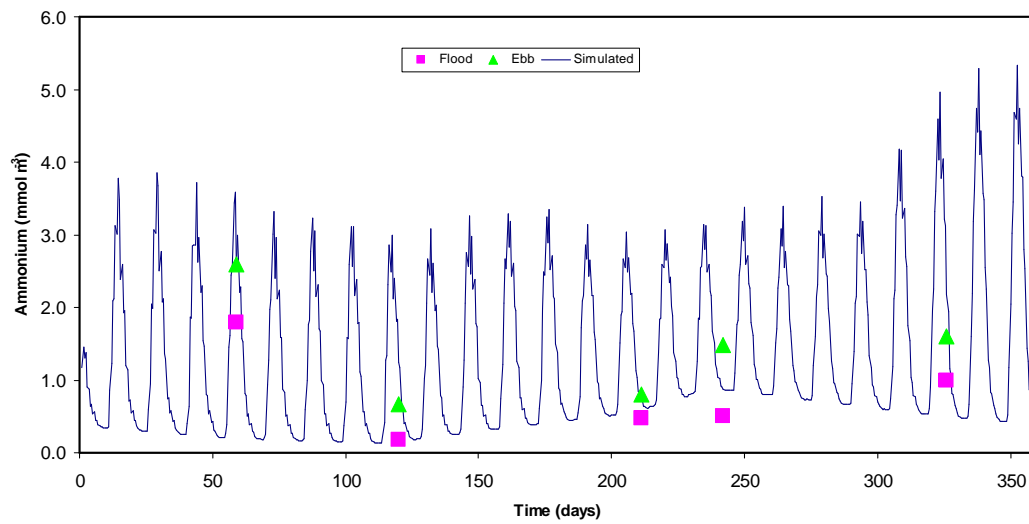
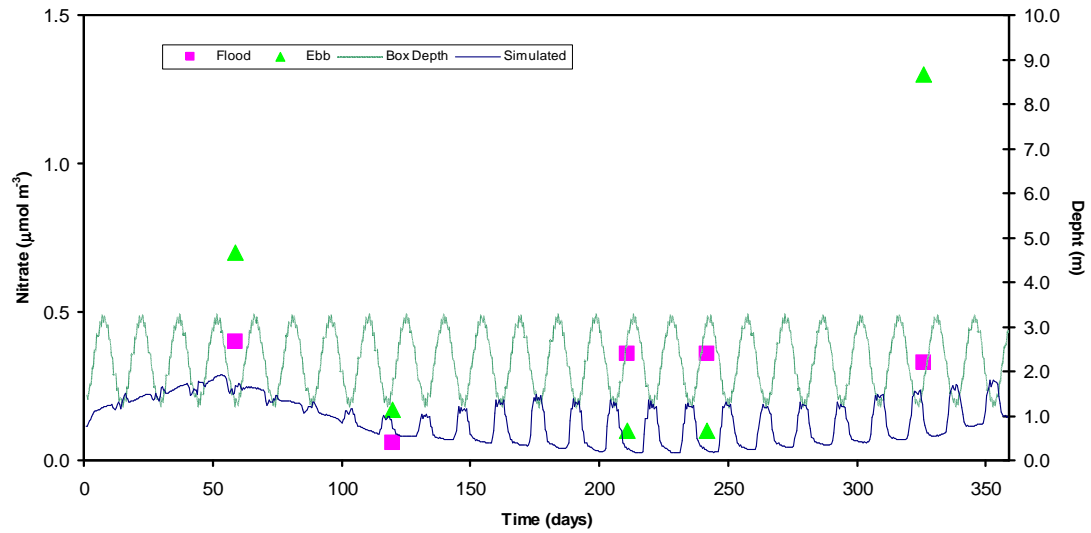


Fig 3-1- Simulated and observed nitrate (upper chart) and ammonia (lower chart) at station RA. Also shown simulated box depth to emphasize the opposite trends between concentration and water depth (upper chart)

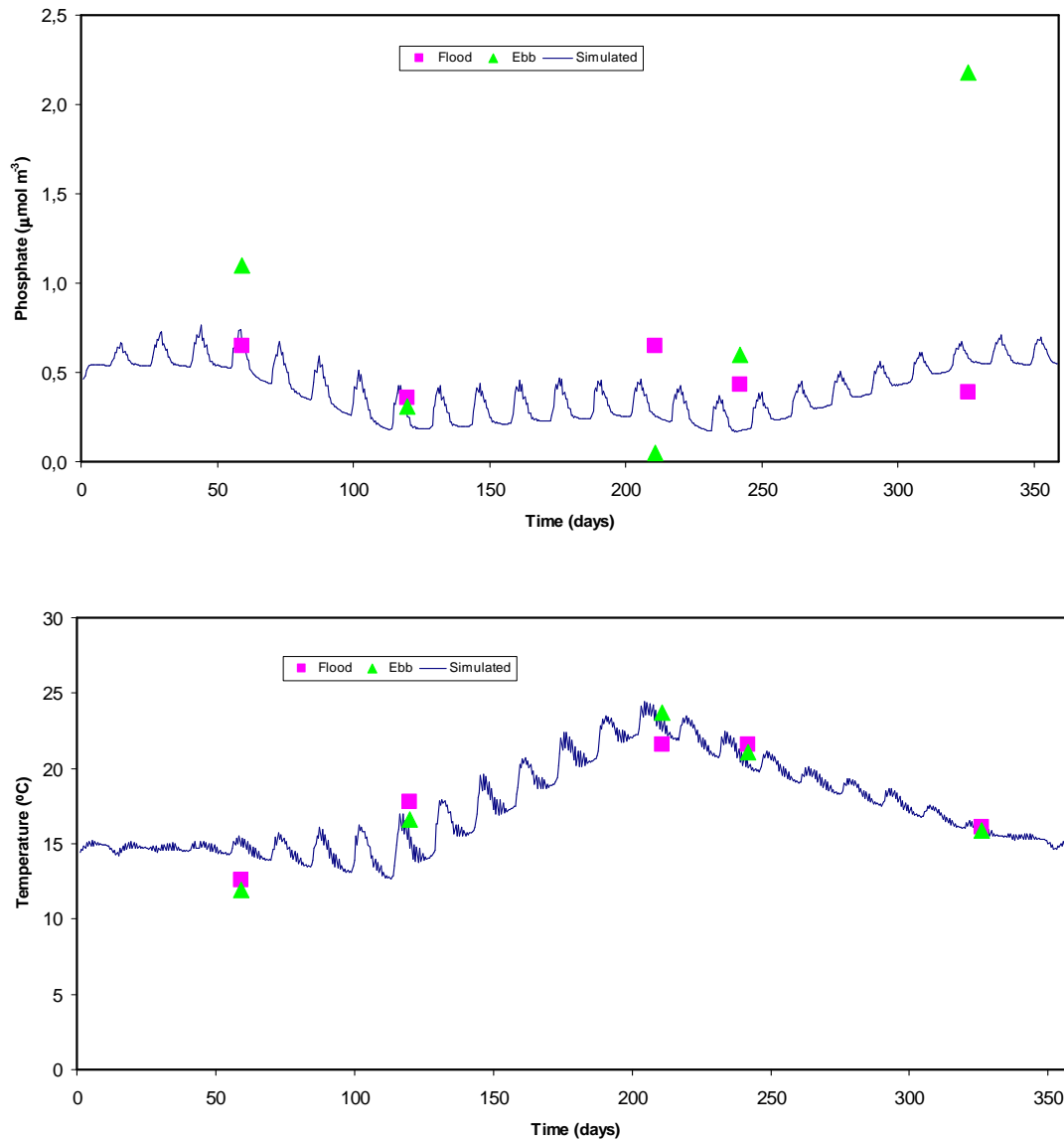


Fig 3-2- Simulated and observed phosphate (upper chart) and water temperature (lower chart) at station RA.

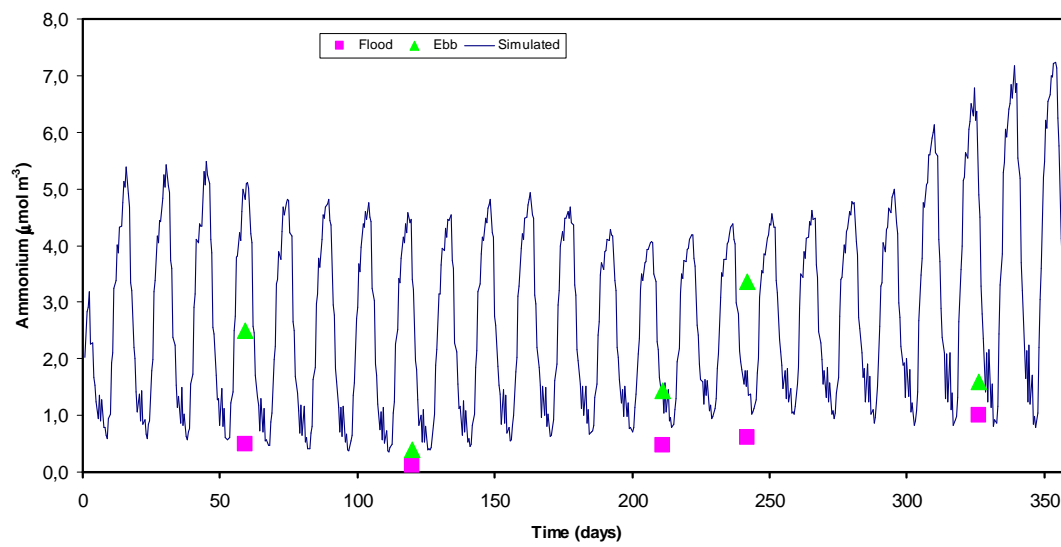
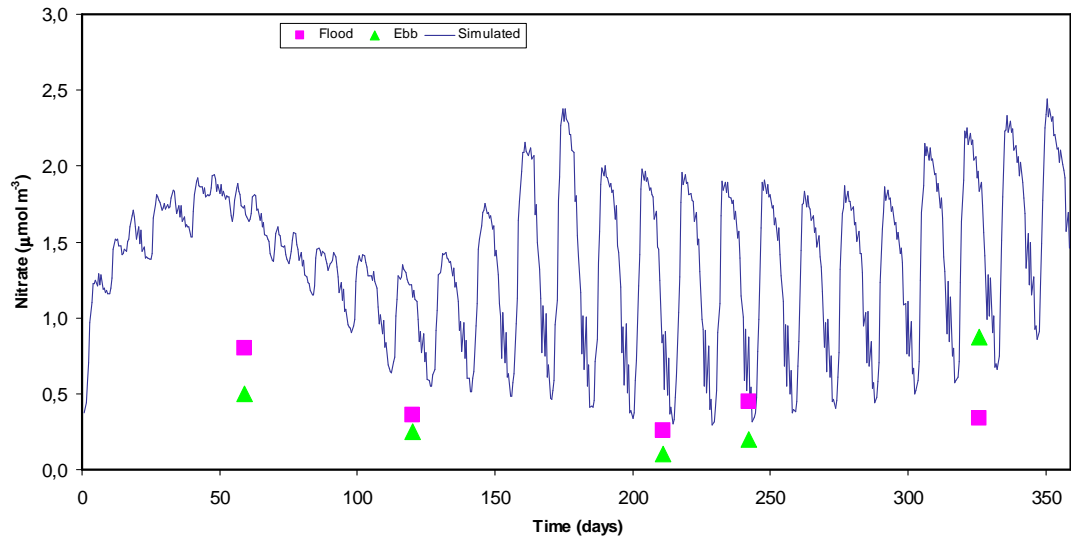


Fig. 3-3 – Simulated and observed nitrate (upper chart) and ammonia (lower chart) at station RB.

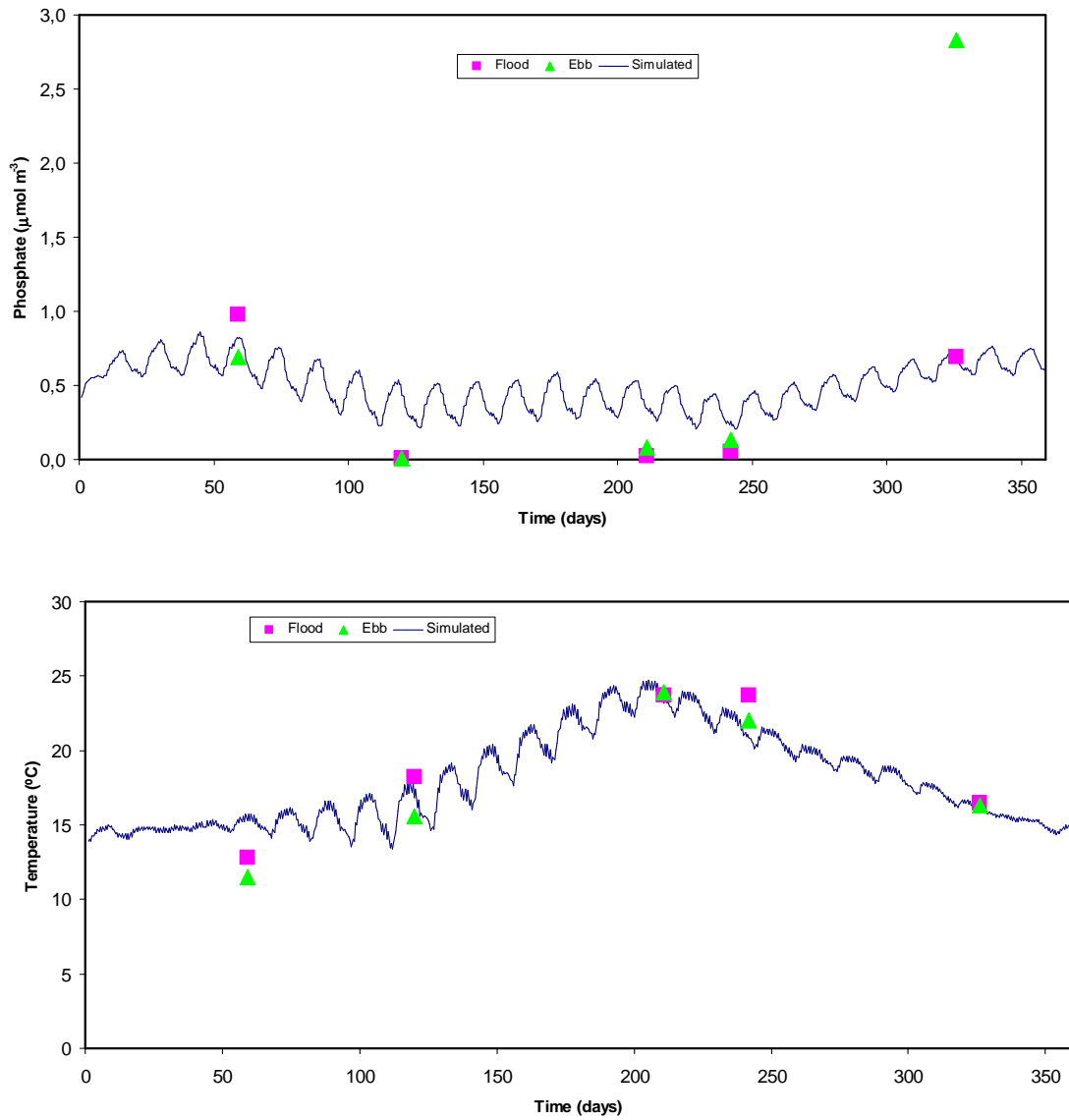


Fig. 3-4 – Simulated and observed phosphate (upper chart) and water temperature (lower chart) at station RB.

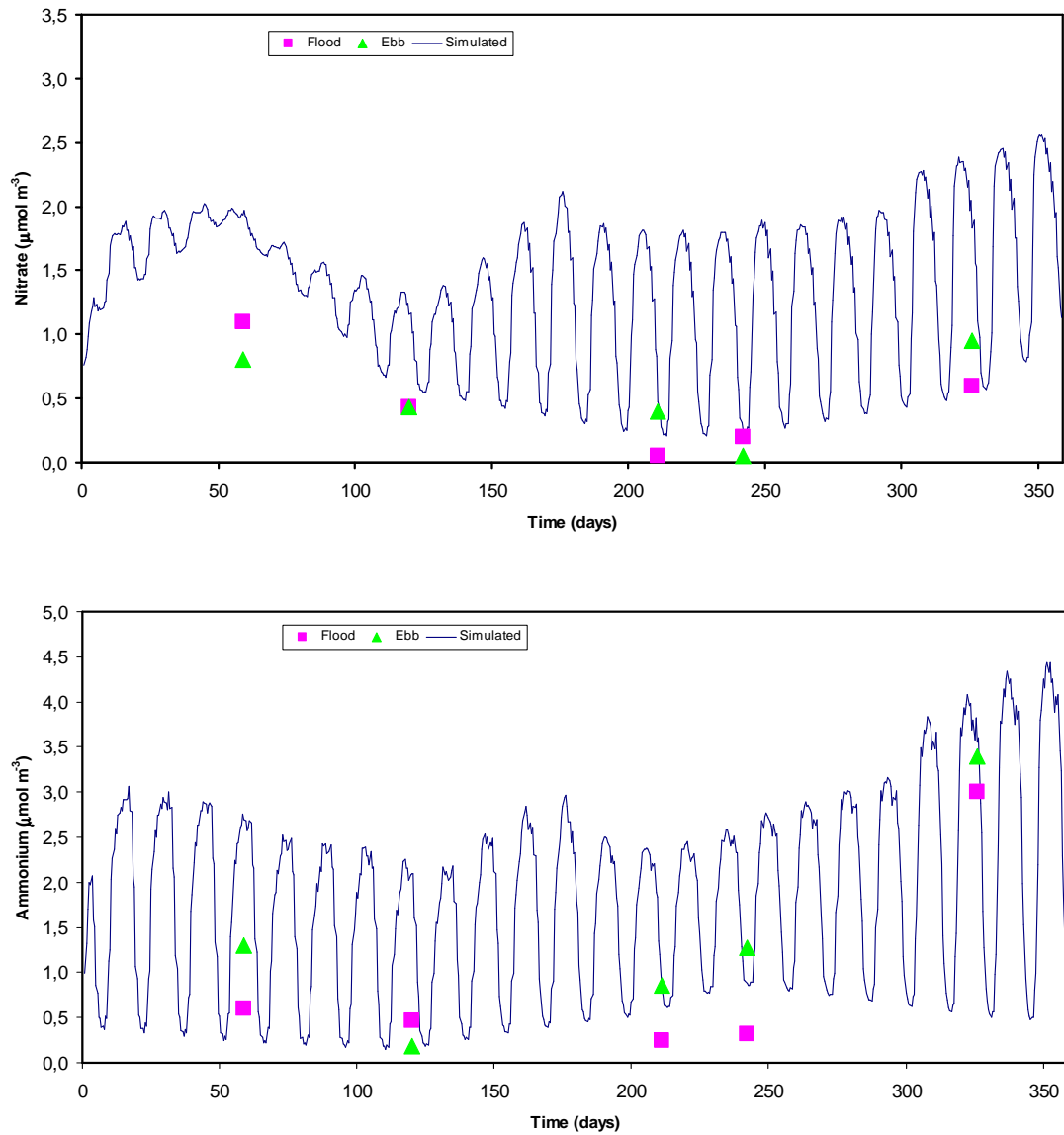


Fig. 3-5 – Simulated and observed nitrate (upper chart) and ammonia (lower chart) at station RC.

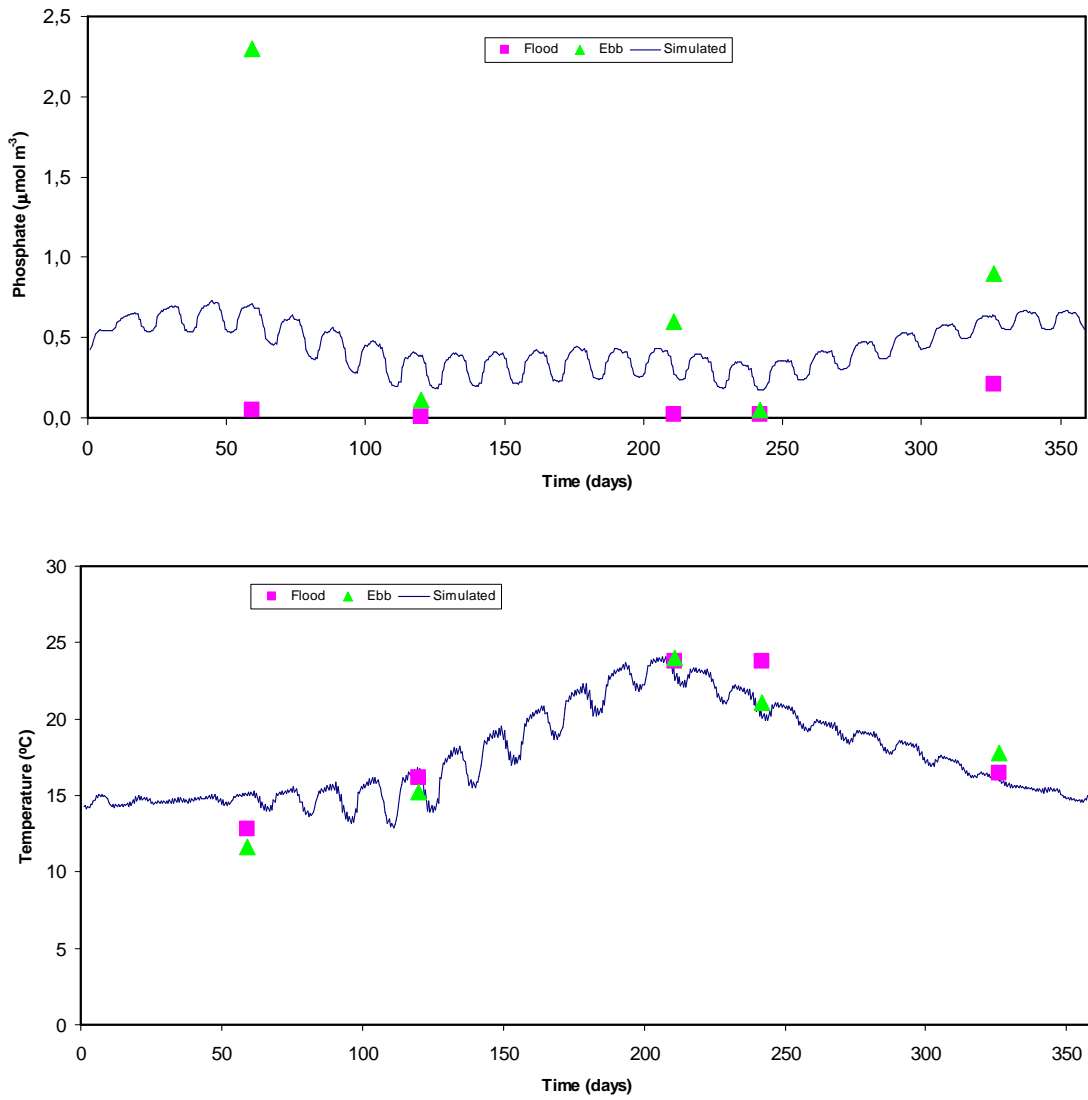


Fig. 3-6 – Simulated and observed phosphate (upper chart) and water temperature (lower chart) at station RC.

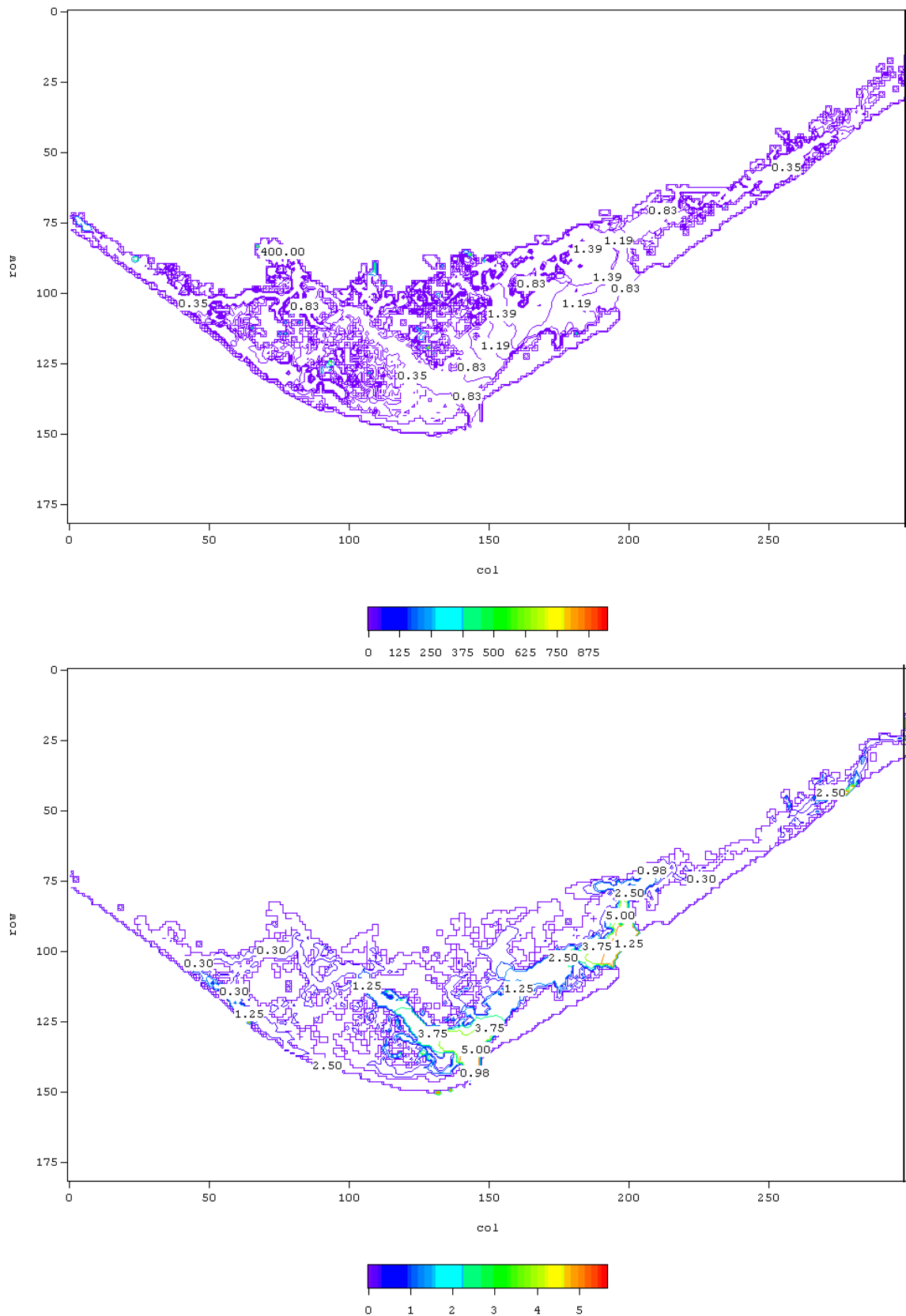


Fig. 3-7 – Example of contour plots showing nitrate (upper figure) in $\mu\text{mol L}^{-1}$ and chlorophyll concentrations (lower figure) in $\mu\text{g L}^{-1}$.

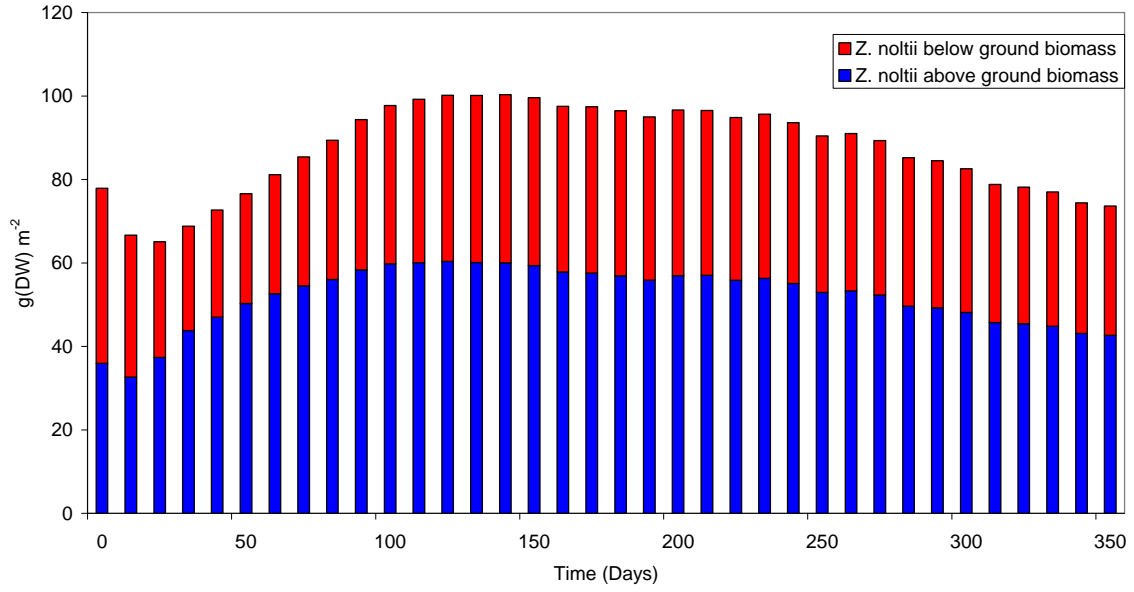


Fig. 3-8 – Simulated average *Z. noltii* above and below ground biomass over its habitat areas (cf. – Fig. 2-5).

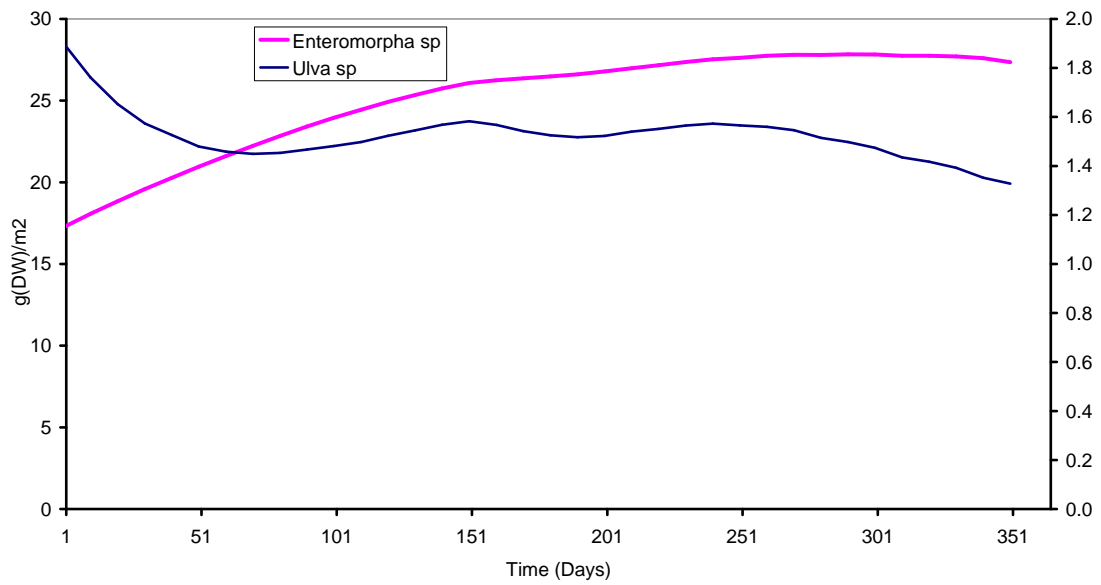


Fig. 3-9 – Simulated average *Enteromorpha* and *Ulva* sp. biomass over its habitat areas (cf. – Fig. 2-5).

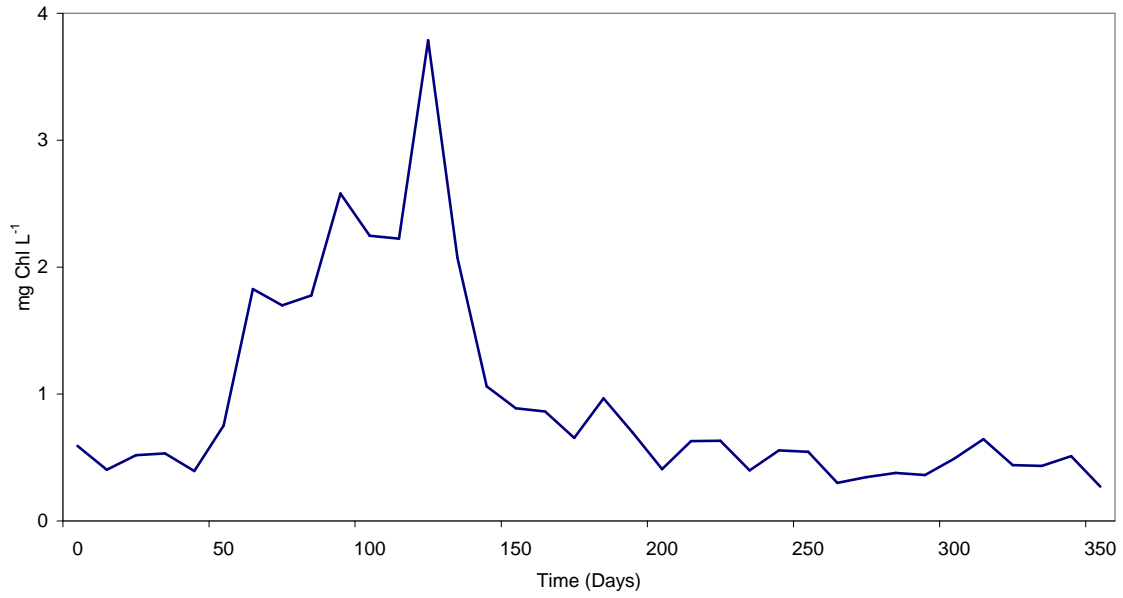


Fig. 3-10 – Simulated average chlorophyll concentration.

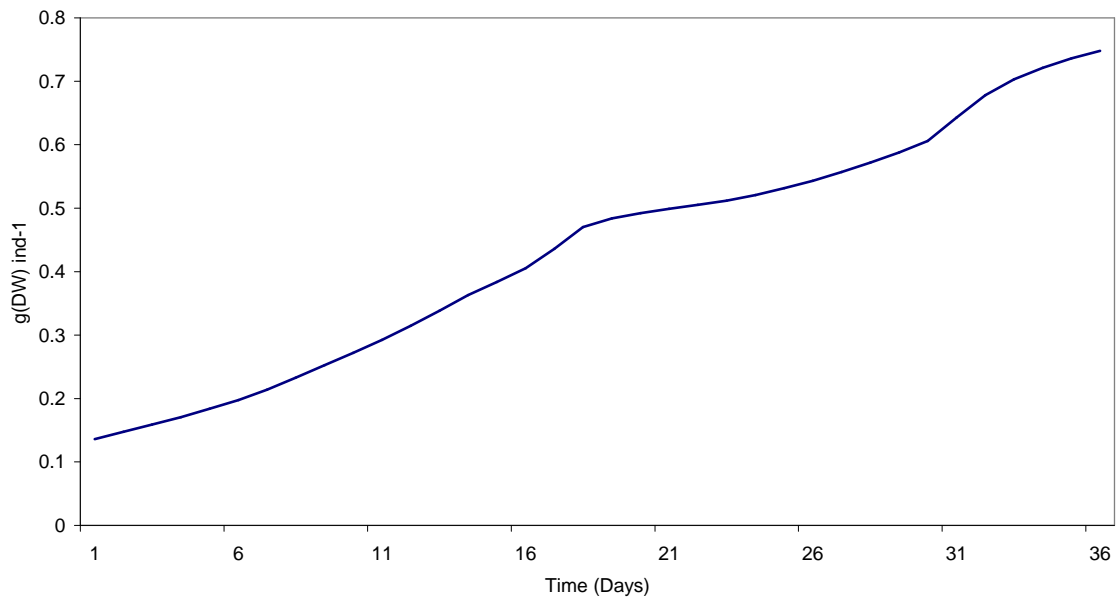


Fig. 3-11 – Simulated average *R. decussates* individual weight biomass over rearing areas (cf. – Fig. 2-6).

Table 3-1 – Sediment and pore water average values (0 – 5 cm), predicted by the model for different sediment types over a period of one year.

	Organic carbon	Organic nitrogen $\mu\text{g g}^{-1}$	Organic phosphorus	Adsorbed phosphorus	Ammonium	Nitrate $\mu\text{mol L}^{-1}$	Phosphate
Mud	7951.85	366.59	161.88	2.80	38.67	0.85	0.95
Muddy-sand	5268.89	192.51	66.87	1.72	39.94	0.81	1.67
Sany-mud	5254.10	175.98	65.01	1.76	39.75	0.93	1.76
Sand	2851.39	76.38	20.53	2.38	33.53	0.43	1.58

4 References

Aníbal, J., 1998. Impacte da macroepifauna sobre as macroalgas Ulvales (Chlorophyta) na Ria Formosa. MSc Thesis. Coimbra University, 73 pp.

Brock, T.D., 1981. Calculating solar radiation for ecological studies. *Ecol Modelling* 14, 1 - 9.

Burns, L.A., 2000. Exposure analysis modelling system (EXAMS): User manual and system documentation. U.S. Environmental Protection Agency.

Chapelle, A., 1995. A preliminary model of nutrient cycling in sediments of a Mediterranean lagoon. *Ecological Modelling* 80: 131-147.

Chapelle, A., Ménesguen, A., Deslous-Paoli, J.M., Souchu, P., Mazouni, N., Vaquer, A. and B. Millet, 2000. Modelling nitrogen, primary production and oxygen in a Mediterranean lagoon. Impact of oysters farming and inputs from the watershed. *Ecological Modelling* 127: 161-181.

Cochlan, W. P. & P.J. Harrison, 1991. Uptake of nitrate, ammonium, and urea by nitrogens-starved cultures of *Micromonas pusilla* (Prasinophyceae): transient responses. *J. Phycol.*: 673-679.

Duarte, P., Meneses, R. , Hawkins, A.J.S., Zhu, M., Fang, J. and J. Grant, 2003. Mathematical modelling to assess the carrying capacity for multi-species culture within coastal water. *Ecological Modelling* 168: 109-143.

Duarte, P., Azevedo, B. and A. Pereira, 2005. Hydrodynamic Modelling of Ria Formosa (South Coast of Portugal) with EcoDynamo. DITTY report. Available at <http://www.dittyproject.org/Reports.asp>.

Ducobu, H., Huisman, J., Richard, Jonker, R. & L.R. Mur, 1998. Competition between a Prochlorophyte and a Cyanobacterium under various phosphorus regimes: comparison with the droop model. *Journal of Phycology*: 467-476.

Falcão, M.M., 1996. Dinâmica dos nutrientes na Ria Formosa: efeitos da interacção da laguna com as suas interfaces na reciclagem do azoto, fósforo e sílica. PhD, University of Algarve.

Falcão, M, Duarte, P., Matias, D., Joaquim, S., Fontes, T. & R. Meneses, 2000. Gestão do cultivo de bivalves na Ria Formosa com recurso à modelação matemática. IPIMAR.

Falcão, M, L. Fonseca, D. Serpa, D. Matias, S. Joaquim, P. Duarte, A. Pereira, C. Martins & M.J. Guerreiro, 2003. Synthesis report. Available at <http://www.dittyproject.org/Reports.asp>.

Ferreira, J., Duarte, P. & B. Ball, 1998. Trophic capacity of Carlingford Lough for aquaculture - analysis by ecological modelling. *Aquatic Ecology*, 31 (4): 361 – 379.

Grant, J., & C. Bacher, 2001. A numerical model of flow modification induced by suspended aquaculture in a Chinese Bay. *Can. J. Fish. Aquat. Sci.* 58: 1 - 9.

Guerreiro, M.J. & C. Martins, 2005. Calibration of SWAT Model: Ria Formosa Basin (South Coast of Portugal). DITTY report. Available at <http://www.dittyproject.org/Reports.asp>.

Hawkins, A. J. S., Bayne, B.L., Bougrier, S., Héral, M., Iglesias, J.I.P., Navaro, E., Smith, R.F.M. & M.B. Urrutia, 1998. Some general relationships in comparing the feeding physiology of suspension-feeding bivalve molluscs. *Journal of Experimental Marine Biology and Ecology* 219: 87-103.

Jørgensen, S.E. & G. Bendricchio, 2001. Fundamentals of ecological modelling. *Developments in Ecological Modelling* 21. Elsevier, Amsterdam, 530 pp.

Jørgensen, S.E., Nielsen, S. & L. Jørgensen, 1991. *Handbook of Ecological Parameters and Ecotoxicology*. Elsevier, Amsterdam, 1263 pp.

Knauss, J.A. 1997. *Introduction to physical oceanography*. Prentice-Hall.

Langdon, C., 1993. The significance of respiration in production measurements based on oxygen. *ICES mar. Sci. Symp.* 197, 69-78.

Mann, K.H. & J.R.M. Lazier, 1996. *Dynamics of marine ecosystems*. Blackwell Science.

Neves, R.J.J., 1985. Étude expérimentale et modélisation mathématique des circulations transitoire et résiduelle dans l'estuaire du Sado. Ph.D. Thesis, Université de Liège.

Parsons, T.R., Takahashi, M., & B. Hargrave, 1984. *Biological oceanographic processes*. 3rd. Edition. Pergamon Press.

Pereira, A. & P. Duarte, 2005. EcoDynamo Ecological Dynamics Model Application. University Fernando Pessoa. DITTY report. Available at <http://www.dittyproject.org/Reports.asp>.

Plus, M., Chapelle, A., Ménesguen, A., Deslous-Paoli, J.-M. & I. Auby, 2003. Modelling seasonal dynamics of biomasses and nitrogen contents in a seagrass meadow (*Zostera noltii* Hornem.): application to the Thau lagoon (French Mediterranean coast). *Ecological Modelling* 161: 213-238.

Portela, L.I. & R. Neves, 1994. Modelling temperature distribution in the shallow Tejo estuary. In: Tsakiris and Santos (Editors), *Advances in Water Resources Technology and Management*, Balkema, Rotterdam, pp. 457 - 463.

Raillard, O., Deslous-Paoli, J.-M., Héral, M. & D. Razet, 1993. Modélisation du comportement nutritionnel et de la croissance de l'huître japonaise *Crassostrea gigas*." *Oceanologica Acta* 16: 73-82.

Raillard, O. & A. Ménesguen, 1994. An ecosystem box model for estimating the carrying capacity of a macrotidal shellfish system. *Marine Ecology Progress Series* 115: 117-130.

Rodrigues, A. Carvalho, A., Reia, J., Azevedo, B., Martins, C., Duarte, P., Serpa, D. & M. Falcão, 2005. A geographical information system for Ria Formosa (South coast of Portugal). DITTY report. Available at <http://www.dittyproject.org/Reports.asp>.

Santos, R., Sprung, M., Machás, R., Aníbal, J., Dias, N., Mata, L., Vieira, V., Piedade, F., Pérez-Lloréns, L., Hernández, I., Vergara, J. & G. Peralta, 2000. Relatório final do projecto “Produção bentónica e fluxos de matéria orgânica na Ria Formosa, Algarve, Portugal. Relatório final do projecto contracto nº 12/REG/6196.

Serpa, D., 2004. Macroalgal (*Enteromorpha* spp. and *Ulva* spp.) primary productivity in the Ria Formosa lagoon. Master thesis, Faculty of Science and Technology, New University of Lisbon.

Service Hydrographique et Océanographique de la Marine (SHOM), 1984. Table des marées des grands ports du Monde. Service Hydrographique et Océanographique de la Marine, 188 pp.

Sobral, M.P.O., 1995. Ecophysiology of *Ruditapes decussatus* L. (Bivalvia, Veneridae). PHD thesis, Universidade Nova de Lisboa.

Solidoro, C., Pecelik, G., Pastres, R., Franco, D. & C. Dejak, 1997. Modelling macroalgae (*Ulva rigida*) in the Venice lagoon: Model structure identification and first parameters estimation. *Ecological Modelling*, 94: 191-206.

Steele, J.H., 1962. Environmental control of photosynthesis in the sea. *Limnol. Oceanogr.*, 7: 137-150.

UE (2000). Directiva 2000/60/CE do Parlamento Europeu e do Conselho que estabelece um Quadro de Acção Comunitária no Domínio da Política da Água. J.O.C. de 22.12.2000.

Vollenweider, R.A., 1974. A manual on methods for measuring primary productivity in aquatic environments. Blackwell Scientific Publications.